Venus Express

Radio Science Experiment VeRa

Reference Systems and Techniques Used for the Simulation and Prediction of Atmospheric and Ionospheric Sounding Measurements at Planet Venus

Prepared by

B. Häusler, W. Eidel, D. Hagl, S. Remus, J. Selle, UniBwM

and M. Pätzold, IGM

Approved by

Bernd Häusler (VeRa Principal Investigator)

Document Change Record

Issue	Rev	Sec	Date	Changes	Author
1	0		24.09.2003		Häusler
2	1		11.11.2003		Häusler
2	3		12.11.2003		Häusler
2	4		12.12.2003		Häusler
2	5		23.07.2004	Equation 3.40, 3.42, 3.43	Häusler

DISTRIBUTION LIST

Recipient	Institution	No. of copies
VeRa Team		
Bernd Häusler	Universität der Bundeswehr München	5
Martin Pätzold	IGM, Universität zu Köln	1
M. Bird	University Bonn	1
R. Treumann	Max-Planck-Institut für extraterrestr. Physik, Garching	1
L. Tyler	Stanford University	1
R. Simpson	Stanford University	1
D. Hinson	Stanford University	1
Science Coordinator		
D. Titov	Max-Planck-Institut für Aeronomie, Katlenburg	1
ESTEC / ESOC		
H. Svedhem	ESTEC, Noordwijk	1
R. Schmidt	ESTEC, Noordwijk	1
T. Morley	ESOC, Darmstadt	1
Michel Denis	ESOC, Darmstadt	
Patrick Martin	ESTEC, Noordwijk	
H. Eggel	ESTEC, Noordwijk	1
POS	Payload Operation Service, Rutherford	
JPL / NAIF		
Ch. H. Acton	Jet Propulsion Laboratory, Pasadena	
N. Bachman	Jet Propulsion Laboratory, Pasadena	
EADS-Astrium		
A. Clochet	EADS-Astrium	1

ACRONYMS

CEP	Celestial Ephemeris Pole
CTP	Conventional Terrestrial Ploe
CL	Closed Loop Reception at GS
ESA	European Space Agency
ET	Ephemeris Time
FD	Flight Dynamics ESOC
GHA	Greenwich Hour Angle
GMST	Greenwich Mean Sidereal Time
GMT	Greenwich Mean Time
GRT	General Relativity Theory
G/S	Ground Station
HGA	High Gain Antenna of the Satellite
HK	Housekeeping Data
IAU	International Astronomical Union
ICRS	International Celestial Reference System
IERS	International Earth Rotation Service
ITRS	International Terrestrial Reference System
JD	Julian Date
MaRS	Mars Express Radio Science Experiment
MCS	Mission Control System ESOC
MEX	Mars Express Orbiter
MJD	Modified Julian Date
NAIF	Navigation and Ancillary Information Facility
OBD	Spacecraft Onboard Time
OL	Open Loop Reception at GS
ONES	One Way Single Frequency Transmission Mode (non coherent)
ONED	One Way Dual Frequency Transmission Mode (non coherent)
RSS	Radio Science Simulator

S/C	Spacecraft
TAI	International Atomic Time
TCG	Geocentric Coordinate Time
TDB	Barycentric Dynamic Time
TDT	Terrestrial Dynamical Time = TT
TEC	Total Electron Content
TM	Telemetry
TWOS	Two Way Single Frequency Transmission Mode (coherent)
TWOD	Two Way Dual Frequency Transmission Mode (coherent)
TT	Terrestrial Time = TDT
UniBw	Universität der Bundeswehr München
UT1	Universal Time
UT	Coordinated Universal Time
VEX	Venus Express

Contents

1. INTRODUCTION

Venus Express is an ESA F-mission devoted to the study of the planet Venus. The spacecraft will be launched by a Soyus Fregat launch vehicle from Baikonur in November 2005 [1.1].

The Venus Express (VEX) mission will be equipped with the radio science experiment VeRa dedicated to study the atmosphere, ionosphere, surface and gravity anomalies of the planet during occultation passes and bistatic radar configurations. VeRa will use the coherent two way dual frequency transmission mode (TWOD). The onboard radio subsystem will contain also an ultrastable oscillator (USO) to allow high precision radio frequency measurements with the onboard S-band/X-band transponder system in the one way dual frequency (ONED) mode. The later will be the preferred transmission mode for occultation and bistatic radar measurements while solar corona and gravity measurements will be carried out using the TWOD mode.

Specifically VeRa will [1.1, 1.2]:

- Determine the atmospheric structure from the cloud deck (35-40 km) to 100 km and derive vertical profiles of neutral mass density, temperature, and pressure as a function of local time and season.
- Localize and determine the temporal and spatial distribution of mid altitude (60 km) atmospheric gravity waves.
- Investigate the spatial and temporal behavior of the H_2SO_4 absorbing layer below the cloud deck.
- Determine the dielectric properties and roughness of the Venusian surface.
- Investigate the ionospheric structure from approx. 80 km to ionopause (600km).
- Study the interaction of solar wind plasma with the Venusian atmosphere/ionosphere as a function of local time, season and solar wind activity.

The primary ground station foreseen to support the radio science measurements will be the ESA New Norcia (NOC) ground station. It is supported for special mission phases by the NASA-JPL- DSN network.

The distribution of the planetary occultation seasons through the VEX mission time is shown in **Fig. 1-1**.

We treat in this document especially the prediction and simulation of planetary occultation experiments, but mention also the reconstruction of an attitude manoeuvre based on S/C housekeeping data. The radio frequency signal characteristics and observables (Doppler frequency shift, ranging delay) which will be measured at the G/S have to be predicted with high accuracy to allow the later extraction of scientific valuable information from the measured values. Therefore, we focus mainly on three points:

- Definition of time basis and astronomical reference systems in order to predict Doppler effects and ranging time delays at the G/S.

- Definition and simulation of high precision S/C attitude control maneuvers which are required to compensate for atmospheric ray bending effects of the radio frequency signal. (In a similar sense these methods will also apply for the bistatic radar experiments).

- Correction methods to eliminate ground and onboard system errors

Information given must at all times be accurate to ~1 second (absolute) and a 3-axis manoeuver must be accurate to ~0.1° (absolute).

The simulations and predictions for the VeRa experiments will be performed by the Radio Science Simulator (RSS) developed at the Institut für Raumfahrttechnik at UniBwM.

Last but not least this paper shall serve as a guide line for the students working in the Radio Science research area.

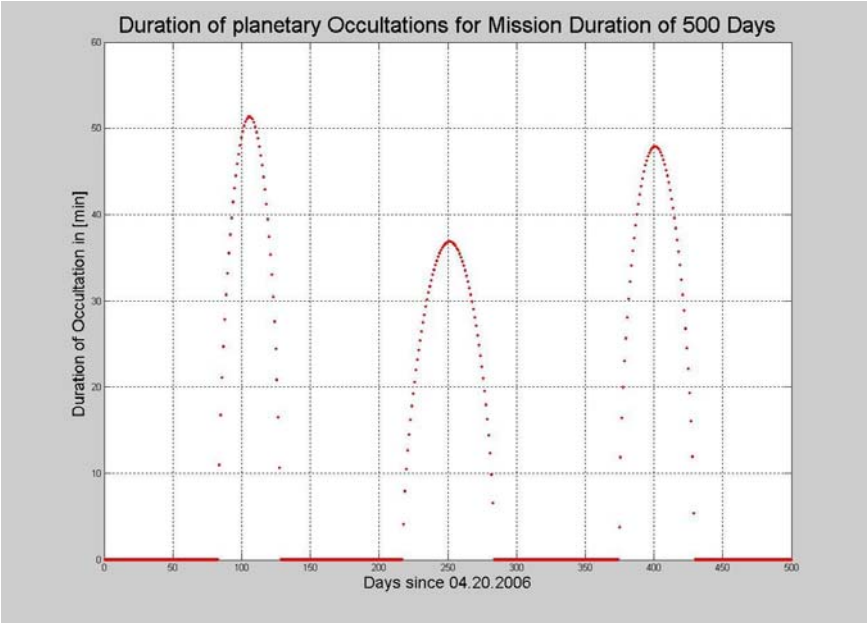

Fig. 1-1: Distribution of planetary occultation seasons during VEX mission time [1.2]

2. Experimental Technique

2.1 Signal Parameters and Physical Factors

Radio Science Experiments are conducted by transmitting high frequency carrier signals between a spacecraft and ground station(s) on Earth. While propagating, the signals are modified as they are influenced by the structures and media they encounter as well as the relative motion between the ground station and spacecraft. Modifications of the signal parameters (including frequency and phase variations with time, signal amplitude, polarization, and delay) are measured and recorded by the ground station.

Table 2.2-1 shows the physical factors that cause variations in the radio signal parameters.

2.2 Onboard and Ground Systems

Transmission of radio signals between the spacecraft and ground station occur through one of two modes. When the spacecraft transmits signals it has generated to the ground station on Earth it is known as One-way mode (ONES/ONED). Two-way mode (TWOS/TWOD) is a configuration whereby signals are generated and transmitted by a ground station on Earth to a spacecraft. The signals are shifted in frequency by the spacecraft's transponder and then sent back to the ground station on Earth (see **Figure 2.2-1**).

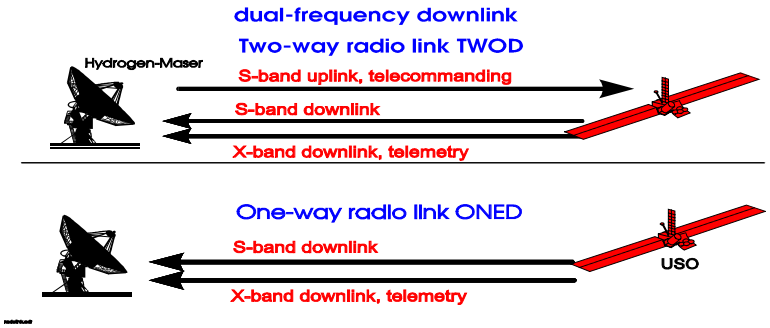

Figure 2.2-1: Transponder Configurations for Radio Science Measurements

For one-way mode the signals are generated by an on-board ultra stable oscillator (USO) with a frequency stability of $\Delta f / f = 10^{-13}$. In the case of two-way mode, the signals are generated by a H_2-Maser located at the ground station with a frequency stability of $\Delta f / f = 10^{-15}$. To preserve

and utilize the H_2-Maser stability, for two-way mode, the signals are coherently converted to the downlink frequency by a transponder before being transmitted back to the ground station on Earth. The stability of the frequency references listed above are critical to radio science experiments since only through their high stability are minute changes in the signal frequency/phase and delay detectable. The VEX spacecraft telecommunication and Telecommand (TT&C) subsystem is shown in **Figure 2.2-2**.

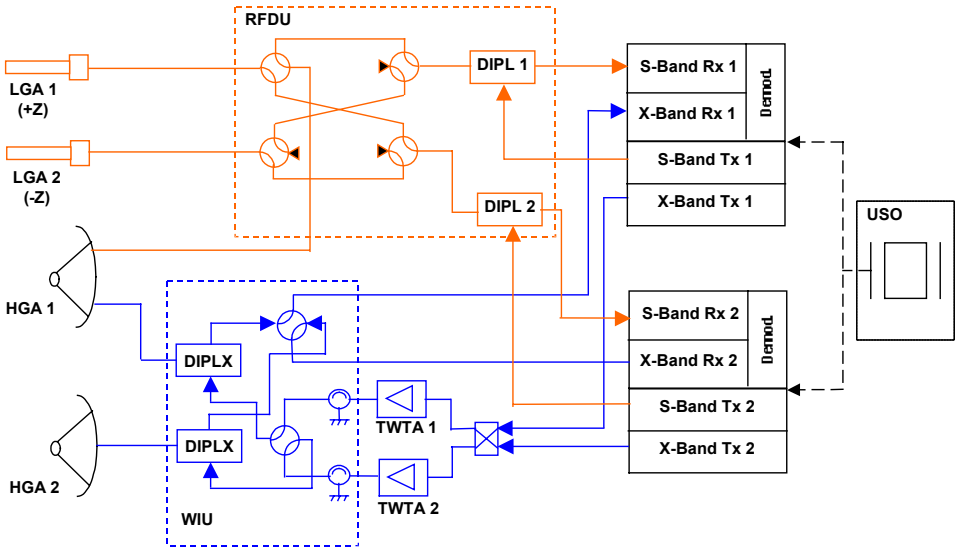

Figure 2.2-2: VEX Spacecraft TT&C Subsystem with Redundant Transponders, USO and a Radio Science Distribution Unit (RFDU) [2.1].

Signals for both the one-way (ONED) and two-way mode (TWOD) will be undesirably modified by the ground station and spacecraft TT&C systems. Since the objective of radio science is to detect the signal modifications from structures and mediums in space, the ground station and spacecraft influences on the signal must be calibrated out of the final radio science data. The Radio Science Team, therefore, will conduct tests on the Venus Express transponder (which is the most influential TT&C component) to determine signal modifications in terms of frequency, frequency stability (Allan Variance), phase noise, spurious responses and group delay. Influences from the ground stations are supplied by the specific ground station involved in the form of calibration data (see chapter 7).

The configuration of the ground station has to be such that for the occultation experiments the receiver works in an open loop mode (OL), receiving simultaneously in X- and S-band, while for the bistatic radar experiments the signals have to be received additionally in two polarities either in X-band or in S-band frequency. Ranging has to be performed in TWOD mode (see Table below) in order to be able to extract TEC values. (see below)

Table 2.2-1: Physical Factors, Transmission Mode and Ground Station Configuration for VeRa

Occultation	Atmospheric density, temperature and pressure profiles. Ionospheric structure. H2SO4 absorbing layer	ONED USO driven Carrier only	OL	X + S down
Bistatic Radar	Planetary surface dielectric properties and roughness	ONES USO driven Carrier only	OL	X and S down both polarizations
Solar Corona	Solar corona structure, interaction of solar wind plasma with planetary atmosphere/ionosphere	TWOD coherent	CL, OL	S up X+S down both polarizations
Gravity	Gravity anomalies	TWOD coherent Carrier only	CL	X up X+S down
Dual frequency Ranging	Total columnar electron content (TEC)	TWOD coherent Ranging mode	CL	X up X+S down

2.3 Radio Science Measurement Principles

The classical radio science measurement principle is based on the detection of a shift in frequency. This shift in frequency can be due to propagation through a medium (with a specific index of refraction, n) and/or the relative motion between the sender and receiver (classic Doppler).

Deriving the shift in frequency begins by defining the optical path length. The optical path length for an electromagnetic wave is dependent on two factors: the index of refraction, n, and the actual path over which the wave travels through the medium, dl_1. The general equation for the optical path length, L_1, for an electromagnetic wave within a medium is as follows:

$$L_1 = \int n \; dl_1$$

where:

$L_1 = \text{path length through medium}$

$n = \text{index of refraction}$

$dl_1 = \text{integration path in medium}$ (2.3.1)

The refractive index, n, and all n dependent equations, refer to phase (as apposed to group) parameters since n is based on the phase velocity ($n = c / v_{phase}$).

For a vacuum, this actual path length is a straight line between the sender and receiver. In a medium where n ≠ 1, however, the rays are bent, causing a longer actual path length than that of a straight line, shown in **Figure 2.3-1**.

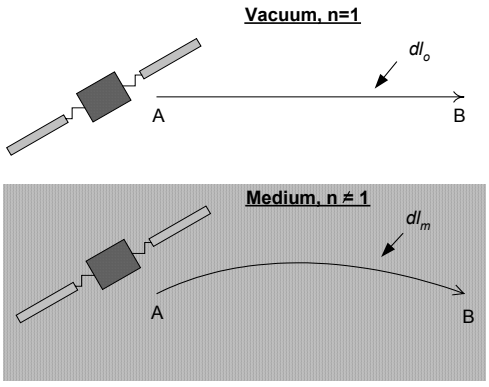

Fig.: 2.3-1: Depiction of a ray traveling through a vacuum and through a medium; whereby the direction of the ray in the medium is constantly changing (bending) due to the variation of n with position.

By then formulating a theoretical comparison of the optical path length experienced by the electromagnetic wave through the medium to that of a vacuum, the effects of the medium can be isolated. The difference in optical path length in the vacuum and the medium then represents the increase in optical path length due to the medium only, not the overall distance traveled.

$$\begin{aligned}\Delta l_m &= L_m - L_o \\ &= \int n\, dl_m - \int 1\, dl_o\end{aligned} \tag{2.3.2}$$

As a first order approximation to this comparison, a straight line propagation through the medium can be assumed, i.e. $dl_o = dl_m$ [2.3].

$$\Delta l_m = \int (n-1)\, dl_o \tag{2.3.3}$$

This difference in path length can then be correlated to a difference in phase.

The increase in phase due to the medium is therefore represented by:

$$\Delta\phi_m = \frac{2\pi}{\lambda_o}\int (n-1)\, dl_o \tag{2.3.4}$$

For an ionized medium, the index of refraction n (n<1) is related to the medium's electron number density N_e [m^{-3}] (f_p being the plasma frequency of the medium) and the signal's frequency to second order in f/f_p.

$$n = 1 - \frac{40.3\left[\frac{m^3}{s^2}\right]\cdot N_e}{f^2} \tag{2.3.5}$$

.

The neutral atmosphere, however, is a non-dispersive medium. The index of refraction n (n>1) does not depend on the frequency. Its impact on Earth, the tropospheric refraction, can not be determined with a dual frequency observation as will be shown below for the ionosphere. It will therefore be treated in chapter 7.1 as an effect which has to be corrected for in prediction routines and in the later data analysis.

The change in phase is then correlated to a change in frequency through:

$$\Delta f_m = \frac{1}{2 \cdot \pi} \frac{d(\Delta \phi_m)}{dt} \tag{2.3.6}$$

Combining the equations for $\Delta \phi_m$,n, and Δf_m yields for an ionized medium:

$$\Delta f_m = \frac{-40.3\left[\frac{m^3}{s^2}\right]}{c \cdot f} \cdot \frac{d}{dt} \int N_e \; dl_o$$

$$\text{where:} \tag{2.3.7}$$

$$c = \text{Speed of Light; TEC} = \text{Total Columnar electron content} = I = \int N_e \; dl_o$$

For the general one way example, whereby the system S (satellite, emitter) is transmitting the frequency f_S , and the system E (Earth G/S) receives the frequency f_E , the shift in frequency will contain contributions from the ionized medium as well as the Doppler effect due to the motion of the satellite

$$\Delta F = \Delta f_d + \Delta f_m \tag{2.3.8}$$

In case of a one way downlink the Doppler effect (including its relativistic contributions) can be derived from the following equation [2.16], [2.7],[2.12],[2.13], [2.15]:

$$\boxed{\frac{f_E}{f_S} \approx \frac{1 - \hat{\mathbf{n}} \cdot \boldsymbol{\beta}_E + \frac{1}{2}\beta_E^2 - \phi_E / c^2}{1 - \hat{\mathbf{n}} \cdot \boldsymbol{\beta}_S + \frac{1}{2}\beta_S^2 - \phi_S / c^2}} \tag{2.3.9}$$

which can be approximated by:

(2.3.10)

$$\boxed{\Delta f_d = f_S - f_E = f_S \left\{ \hat{\mathbf{n}} \cdot (\boldsymbol{\beta}_E - \boldsymbol{\beta}_S) + \frac{1}{2}\left(\beta_S^2 - \beta_E^2\right) + (\hat{\mathbf{n}} \cdot \boldsymbol{\beta}_S)(\hat{\mathbf{n}} \cdot \boldsymbol{\beta}_E) - (\hat{\mathbf{n}} \cdot \boldsymbol{\beta}_S)^2 - \frac{1}{c^2}(\phi_S - \phi_E) \right\}}$$

Here, we define the satellite/transmitter S and the receiver E and $\boldsymbol{\beta} = \mathbf{v} / c$ with $\hat{\mathbf{n}}$ being a unit vector which is pointing from (*S*) to (E*),* i.e. in the direction of the signal propagation. $\mathbf{v}_S$ is the coordinate velocity of the platform (satellite) S and $\mathbf{v}_E$ the coordinate velocity of platform (G/S). The coordinate system used can be a heliocentric or barycentric system. The velocities, however, must be adopted to the selected coordinate system.

If, for example, the velocity of an object needs to be calculated in the coordinates of the barycentric frame we must derive it as a relative velocity from components already determined in another frame (for example as the satellite velocity in a planetocentric frame). Here we agree to the convention that relative velocities can be obtained by simple addition or subtraction of velocity vectors without applying the Lorentz transformation of velocities. (A consideration of the Lorentz transformation would lead us to correction terms of the order $(v/c)^3$ which we will neglect).

The last term in equation (2.3.10) is caused by effects of General Relativity (see also chapter 7.3). Φ_E and Φ_S are the gravitational potentials of E and S. In general, the gravitational potential Φ is given by

$$\Phi = -\frac{GM}{r} \tag{2.3.11}$$

G and M being the gravity constant and the mass of the planetary object.

Knowing the sensitivity with which the Doppler frequency shift can be measured (1mHz) it becomes clear that relativistic corrections must be considered.

Light Time Correction

An important correction has still to be introduced: When determining the velocity vectors in equation (2.3.9) from the ephemeris data we have to include the effect of finite speed of light (light travel time). In case of a planetary mission the velocity vectors of systems S and E are continuously changing and can obtain substantially different values during a light travel time of many minutes. In order to compute the expected Doppler frequency shift correctly, we have to distinguish between two time instants, t_0 and t_1 .

t_0 being the time when the radio wave is emitted

t_1 being the time when the radio wave is received

In order to have platform E (G/S) receive the radio wave at $t = t_1$ it has to be emitted from the S/C (platform S) at $t = t_0$. When the signal is being received on Earth (at platform E) at time t_1, the velocity vectors in equation for E and S have to be taken at different instances of time.

The same argument applies of course for a pure uplink transmission which means that in case of a coherent two way mode transmission both Doppler shifts - detected as well at the S/C receiver as at the G/S receiver - have to be considered [2.14]. The formula for the expected

Doppler shift in the two way mode due to the effect of General Relativity is derived in [2.14, p.60].

Fig. 2.3-2 shows the scenario for a two way measurement indicating that both the S/C motion and the G/S motion have to be considered. The velocity of the G/S must include not only the contribution of the Earth´s translatory motion in inertial space but also the velocity component due to the Earth´s rotation. The rotational speed is given in degrees/second by equation (3.6). (For computation of the Earth velocity in the geocentric ICRS see chapter 3.3.6)

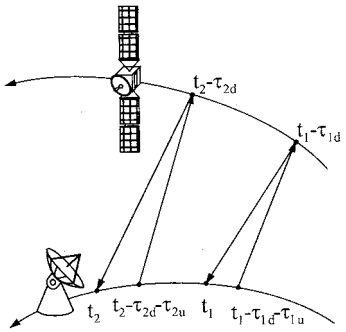

Fig. 2.3-2: The motion of the satellite and the ground station during signal travel time for two-way Doppler measurements [3.1]

$$t_1 - \tau_{1d} - \tau_{1u} = t_0$$

2.4 Occultation Experiments

Occultation is a method used to study planetary atmospheres. It is implemented when, as seen from Earth, the spacecraft disappears behind the planet (Ingress) or the spacecraft emerges from behind the planet (Egress). During these two phases of the spacecraft's orbit the radio signals pass through the planet's atmosphere and are received by the ground station. The signal parameters undergo modifications due to the neutral and ionised regions of the atmosphere. These modifications are measured and analysed to characterize the planetary atmosphere.

Additionally, the two-frequency technique will be employed by Venus Express, whereby two signals are transmitted simultaneously from the S/C in the ONED mode using the USO as the onboard reference frequency. With this technique dispersive plasma effects are separable from nondispersive refractive effects of the neutral atmosphere [2.3]. The geometry used for this method is shown in **Figure 2.4-1**.

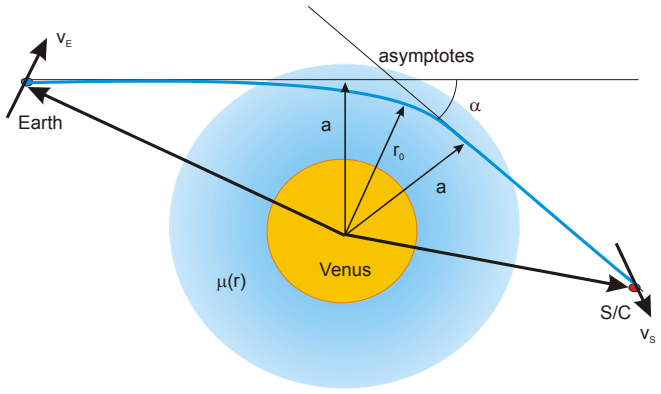

Figure 2.4-1: Geometry used for calculation of an electromagnetic wave refraction in the Atmosphere of Venus during an occultation

The differential Doppler frequency from two different but ratio related frequencies (3/11 in case for S/X –band) for one-way propagation is defined by:

$$\Delta f_{dual} = \Delta F_S - \frac{3}{11}\Delta F_X$$

where:

ΔF_S = frequency shift experienced by S-Band

ΔF_X = frequency shift experienced by X-Band

(2.4.1)

This leads to:

$$\Delta f_{dual} = \frac{-40.3\left[\frac{m^3}{s^2}\right]}{c} \cdot f_S \left(\frac{1}{f_S{}^2} - \frac{1}{f_X{}^2} \right) \cdot \frac{d}{dt} \int N_e \, dl_o \qquad (2.4.2)$$

The dual frequency, first order approximation derivation above shows that the nondispersive refractive effects (classical and relativistic Doppler including General Relativity) are eliminated with this self-calibrating method.

The above derivation uses the straight line first order approximation for the propagation. Section 5 covers the method of ray tracing where this approximation is not made and ray bending is taken into account. The occultation scenario including time basis and light travel time effects is described in Section 3.6.

2.5 Bistatic Radar Experiments

Bistatic Radar is a method used to study remotely the physical characteristics of a specific target at the surface of a planet. For planetary studies the signal is transmitted by a spacecraft toward the planet's surface. The attitude of the S/C is changed such that the specularly reflected radio beam can be received at the ground station **(Fig. 2.5-1)**. The received signal power at two polarities yields information about the dielectric constant of the planetary surface and spectral behaviour yields information about the surface structure on scales smaller than the wavelength [2.4]. Attenuation and ray bending effects in the atmosphere must be additionally considered and will be treated in chapter 4.

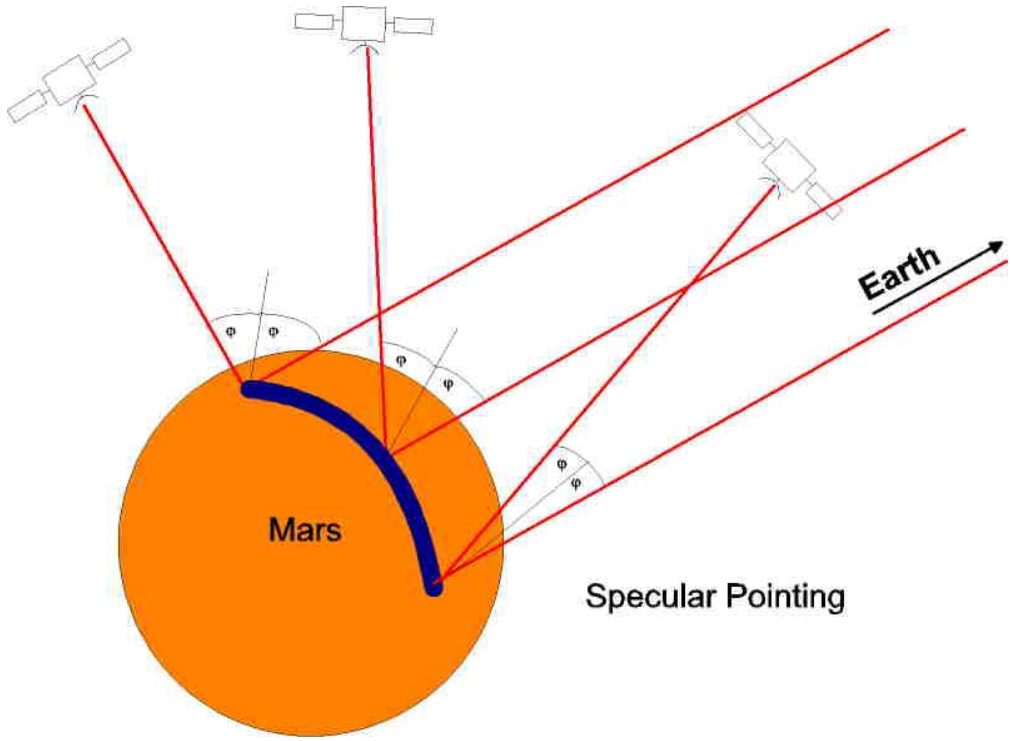

Fig. 2.5-1: Bistatic radar experiment for the case of specular reflection

2.6 Solar Corona/SolarWind

The solar corona experiment is implemented when the spacecraft antenna is pointed toward the Earth. The experiment will last several hours in order to identify plasma turbulence and propagation effects of CME´s in the extended solar corona and will be done in the TWOD mode using the ground station H_2 Maser as reference frequency . The observables are the Doppler frequency shift and the group time delay.

2.6.1 Doppler Measurements /Phase Delay

The total phase time delay T_{phase} is derived from the phase dependent equations above: Δl_m and n:

$$T_{phase} = \tau_{vacuum} + \Delta\tau_{m,phase}$$
$$T_{phase} = \frac{L_1}{c} + \frac{1}{c}\Delta l_m \qquad (2.6.1)$$
$$T_{phase} = \frac{L_1}{c} - \frac{40.3\left[\frac{m^3}{s^2}\right]}{c \cdot f^2}\int N_e \; dl_o$$

where $\Delta\tau_{vacuum}$ = phase delay in vacuum, i.e. delay due to distance traveled

$\Delta\tau_{m,phase}$ =phase delay due only to the medium effect

If we use two down link frequencies and measure for each frequency the Doppler frequency shift we can eliminate non-dispersive effects by determining the *Differential Doppler frequency shift.*

$$\Delta f_{dual} = \frac{-40.3}{c}\left[\frac{m^3}{s^2}\right] \cdot f_S\left(\frac{1}{{f_S}^2} - \frac{1}{{f_X}^2}\right)\frac{d}{dt}\left(\int \Delta N_e \cdot dl_o\right) \qquad (2.6.2)$$

It is important to note that the columnar electron content in the above derivations does not represent an absolute value, but a change in electron content since the beginning of the measurement. This is due to the fact that the phase shift can only be measured relative to the phase of the local oscillator at the start of the measurement (due to an ambiguous number of integral cycles of phase along the path) yielding a relative measurement [2.5]. Any contributions of General Relativity can be neglected.

2.6.2 Ranging Measurements (Group Delay) and Relativistic Corrections

Ranging measurements serve two purposes: Tracking and determination of total columnar electron content along the radio signal path. The total columnar electron content TEC can be determined by using the ranging technique in a special mode, the dual frequency mode (TWOD). Tracking data alone can be gained with one frequency in the TWOS mode if this frequency is high enough not to be affected by solar corona plasma. Ranging measurements are conducted by transmitting a sinusoidal carrier signal which is phase modulated with a square wave using a series of codes. The signal is received onboard the S/C , coherently frequency translated and sent back to the G/S. This coding technique enables the absolute elapsed time to be measured since there is no integral phase cycle ambiguity as in the case of phase delay.

The sensitivity of the measurements is so high that effects of General Relativity have to be considered.

To determine the group delay of the encoded signal the increase in group optical path length, $\Delta l_{m,group}$, due to the medium effect only must be derived along with the group refractive index, n_{group}.

The group refractive index for an ionised medium can be related to the phase refractive index through $v_{phase} \cdot v_{group} = c^2$

$$n_{group} = \frac{1}{n} \cong 1 + \frac{40.3\left[\frac{m^3}{s^2}\right] \cdot N_e}{f^2} \tag{2.6.3}$$

The increase in group optical path length due to the ionised medium effect only in a one way transmission mode is

$$\Delta l_{m,group} = \int \left(n_{group} - 1\right)\ dl_o = \frac{40.3}{f^2} \int N_e\ \ dl_o \tag{2.6.4}$$

The total group delay at the time t (expressed in TDB time units) for the down link path case only is then given by the difference

$$T_{group} = UTC(t) - UTC\left(t - \tau_d\right) \tag{2.6.5}$$

$$\mathrm{T}_{group} = \tau_{vacuum} + \Delta\tau_{m,group} + \Delta\tau_{gr} + \Delta\tau_{trans} + \Delta\tau_{G/S} = \frac{L_1}{c} + \frac{40.3}{c \cdot f^2} \int N_e\ \ dl_o + \Delta\tau_{gr} + \Delta\tau_{trop} + \Delta\tau_{G/S} + \Delta\tau_{trans} \tag{2.6.6}$$

where $L_1 = \frac{1}{c}\left(\left|\vec{r}_{S/C}\left(t - \tau_d\right) - \vec{r}_{G/S}\left(t\right)\right|\right)$

$\vec{r}_{S/C}$ and $\vec{r}_{G/S}$ = the solar-system barycentric positions of the S/C and the G/S

$\Delta\tau_{m,group}$ = group delay due only to the medium effect (neutral and ionized media)

$\Delta\tau_{gr}$ = group delay due to the effect of General Relativity (GRT)

$\Delta\tau_{trop}$ = group delay due to the Earth's troposphere (s. chapter 7.1)

$\Delta\tau_{G/S}$ = group delay due to the G/S antenna-receiver-system (s. chapter 7.4)

$\Delta\tau_{trans}$ = group delay of onboard transponder (s. chapter 7.5)

$\Delta\tau_d$ = down link light travel time

Based on this example of a one way link and by implementing again the differential dual frequency method, as in section 2.5, the non-dispersive effects can be eliminated (including also any contributions from GRT), allowing the extraction of the total columnar electron content.

$$\Delta \mathrm{T}_{group} = \frac{40.3\left[\frac{m^3}{s^2}\right]}{c}\left(\frac{1}{f_S{}^2} - \frac{1}{f_X{}^2}\right)\int N_e \cdot dl_o \qquad (2.6.7)$$

where $\Delta \mathrm{T}_{group}$ = differential group time delay

However, as mentioned above, for ranging purposes, the above dual frequency ranging measurements must be conducted in the coherent two-way mode, taking advantage of the H_2 - Maser stability from the ground station. These measurements, therefore, offer considerably higher accuracy in addition to the elimination of non-dispersive effects.

The derivation of this configuration will be shown for S-band uplink /S-band downlink (S/S) and S-Band uplink / X-band downlink (S/X); whereby, the transponder turnaround ratios for Venus Express (and generally for ESA) are $\mathbf{K}_{S/S} = \frac{240}{221}$ for S/S and $\mathbf{K}_{S/X} = \frac{880}{221}$ for S/X where the S/X turnaround is based on the ratio, m, relating S-band to X-band.

The two-way group time delays (round trip) for S/S and S/X are obtained by adding the uplink and downlink group delays using equation (2.6.7) leading to

$$T_{roup} = UTC(t) - UTC(t - \tau_D - \tau_u) \qquad (2.6.8)$$

for S/S:

$$\mathrm{T}_{group,S/S} = \frac{2L_1}{c} + \frac{40.3}{c}\cdot\frac{1}{f_{S\,up}{}^2}\cdot\left[I_U + \left(\frac{221}{240}\right)^2 I_D\right] + \Delta\tau_{gr} + \Delta\tau_{trop} + \Delta\tau_{G/S} + \Delta\tau_{trans} \qquad (2.6.9)$$

where I_U = total columnar electron content TEC for the uplink

I_D = total electron content TEC for the downlink

$f_{S\,up}$ = S-band uplink frequency

Δt_{gr} = delay caused by effects of General Relativity (GRT)

or more precisely

$$\begin{aligned} T_{group,S/S} = & \frac{1}{c}\left(\left|\vec{r}_{S/C}\left(t-\tau_D\right)-\vec{r}_{G/S}\left(t-\tau_D-\tau_u\right)\right|\right)+\frac{1}{c}\left(\left|\vec{r}_{G/S}\left(t\right)-\vec{r}_{S/C}\left(t-\tau_d\right)\right|\right)+ \\ & +\frac{40.3}{c}\cdot\frac{1}{f_{s\,up}^2}\left[I_U+\left(\frac{221}{240}\right)^2 I_D\right]+ \\ & +\Delta\tau_{gr\,u}+\Delta\tau_{trop\,u}+\Delta\tau_{G/S}+\Delta\tau_{trans}+ \\ & +\Delta\tau_{gr\,d}+\Delta\tau_{trop\,d}+\Delta\tau_{G/S} \end{aligned} \qquad (2.6.10)$$

for S/X:

$$\mathrm{T}_{group,\,S/X}=\frac{2L_1}{c}+\frac{40.3}{c}\cdot\frac{1}{f_{S\,up}{}^2}\cdot\left[I_U+\left(\frac{221}{880}\right)^2\cdot I_D\right]+\Delta\tau_{gr}+\Delta\tau_{trop}+\Delta\tau_{G/S} \qquad (2.6.11)$$

with a similar expansion as in (2.6.10) whereby it is assumed that the total columnar electron content is the same along the X-band and S-band downlink ray paths [2.6].

The differential dual frequency method then eliminates the non-dispersive effects (including also any contributions of GRT and most likely also the transponder), and the total columnar electron content I_u (TEC) for the uplink, allowing for the extraction of the total columnar electron content I_D for the downlink signal path by differencing the above two equations.

The two-way, dual frequency differential group delay is then given by

$$\Delta\mathrm{T}_{group}=\frac{40.3}{c}\cdot\frac{1}{f_{S\,up}{}^2}\cdot\left[\left(\frac{221}{240}\right)^2-\left(\frac{221}{880}\right)^2\right]\cdot I_D \qquad (2.6.12)$$

Since presently all ESOC ground stations are not equipped with a dual frequency ranging unit, the TWOS ranging method is used in the MEX mission. If no dual frequency measurements using the differential method are performed the ranging data must be corrected for the effects of the theory of General Relativity (GRT) since these effects can not be eliminated by differencing equations (2.6.9) and (2.6.11).

Fig. 2.6-1 shows the geometric constellation relevant for our analysis.

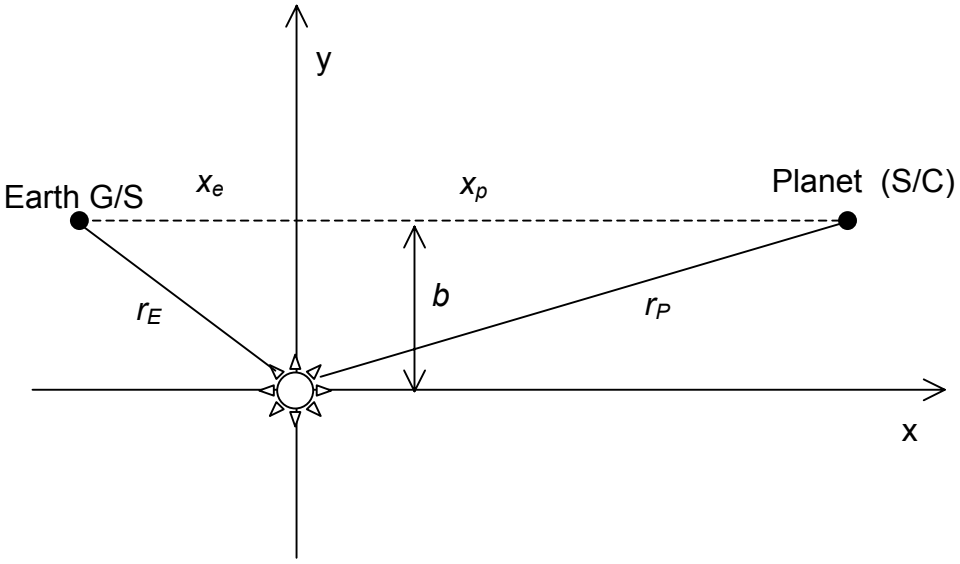

Fig. 2.6-1: Radar echo at planet P (S/C)

Assuming a generalized Schwarzschild metric (where γ is the PPN parameter of General Relativity) we calculate the additional two way delay caused by the gravity field of the sun according to [2.7], [2.8], [2.9], and [2.10] by the following expression:

$$\Delta t_{gr} = \frac{4GM}{c^3}\left[\frac{1+\gamma}{2}\ln\left(\frac{r_e + r_p + \rho}{r_e + r_p - \rho}\right)\right] \sim \frac{2GM}{c^3}\left[(1+\gamma)\,\ln\frac{r_e\, r_p}{b^2}\right] \qquad (2.6.13)$$

ρ, r_e and r_p are the coordinate distances between G/S and planet (satellite), the heliocentric distance of the G/S and the heliocentric distance of the planet (satellite). Useful approximations to this formula are given by Shapiro [2.11].

2.6.3 Spectral Broadening

Spectral broadening is used to determine the solar plasma flow velocity. Spectral broadening arises from the scattering of waves in moving plasma with irregularities. When the spectral line broadening is combined with simultaneous measurements of angular broadening the plasma flow speed can be determined (as shown by Woo [2.7] and summarized by M.K.Bird [2.5]).

The plasma flow speed perpendicular to the line of sight is then

$$v_{\perp} = A \cdot \frac{1}{f} \cdot \frac{\Delta f}{\Delta \theta} \cdot L \tag{2.6.14}$$

where A = constant that depends on such factors as coronal magnetic field strength; etc:

Δf = bandwidth broadening

$\Delta \theta$ = angular broadening

f = signal frequency

and

$$L = \frac{\rho}{\rho - \cos \varepsilon} \tag{2.6.15}$$

where ρ = distance from Earth to Spacecraft in AU

ε = solar elongation angle

3. REFERENCE SYSTEMS AND TIME BASIS - DEFINITIONS

3.1 Time Basis

The scientific success of the VeRa experiments depends critically on a common understanding among ESA, industry, and investigators about the conventions for the reference and time systems. The following chapters shall give an overview about time and coordinate systems which have already been implemented into the radio science software tool (RSS) developed at UniBwM. It is hoped that this document will fertilize and accelerate the process of such a common understanding. An overview on time standards is also given in [3.20].

In the following we have to distinguish among a variety of various time and coordinate systems which are all in use and are selected in practice according to the specific task to be performed. **Figure 3.1-1** will help to understand the basic principles involved.

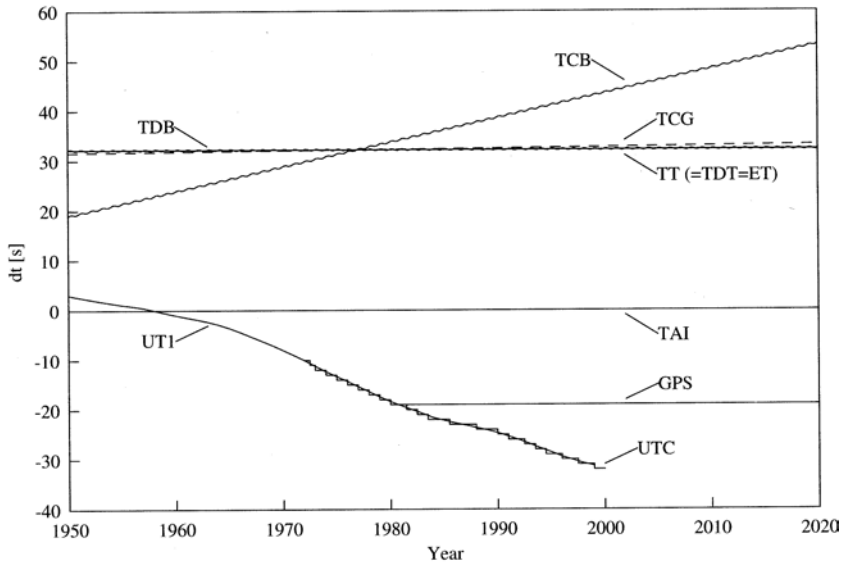

Fig. 3.1-1: Difference of atomic, dynamical, and solar time scales between 1950 and 2020

(The periodic terms of TCB and TDB are magnified by 100 to make them visible) [3.14]

3.1.1 Julian Date (JD)

In astronomical computations, a continuous day count is used which avoids the usage of a calendar. The Julian Date (JD) is the number of days since noon January 1, 4712 BC including fractions of the day.

3.1.2 Modified Julian Date (MJD)

Since the JD has become such a large number, the Modified Julian Date was introduced for convenience. JD was reset at November 17th 1858 which leads to the following equation [3.2]:

$$\mathrm{MJD} = \mathrm{JD} - 2400000.5^{d} \tag{3.1}$$

Note that the count for MJD starts now at midnight.

3.1.3 GMT (UT)

Time is traditionally measured in days of 86400 SI seconds. Each day has 24 hours counted from 0^h at midnight. The motion of the real sun was replaced by the concept of a fictitious mean sun that moves uniformly in right ascension defining the Greenwich Mean Time (GMT) or Universal Time (UT). Greenwich Mean Sidereal Time (GMST), however, is the Greenwich hour angle of the vernal equinox, i. e. it denotes the angle between mean vernal equinox of date and the Greenwich meridian.

The mean vernal equinox is based on a reference system which takes into account the secular effects, i.e. the precession of the Earth´s equator but not periodic effects such as the nutation of the Earth´s axis [3.6, p. 410].

In terms of SI seconds, the length of a sidereal day (i. e. the Earth's spin period) amounts 23^h 56^m $4^s.091 \pm 0^s.005$ (corresponding to a factor 1/1.00273790935) making it about four minutes shorter than a 24^h solar day. Hence, sidereal time and mean solar time have different "rates".

3.1.4 Universal Time (UT1)

Universal Time UT1 is the presently adopted realization of a mean solar time scale (constant average length of a solar day of 24 hours) with UT1 = UT. UT1 is a measurement of the actual rotation of the Earth, independent of observing location. As a result, the length of one second of UT1 is not constant because of the apparent motion of the sun and the rotation of the Earth (see also Fig. 3.1-1). UT1 is therefore defined as a function of sidereal time [3.1].

For any particular day, 0 h UT1 is defined as the instant at which Greenwich Mean Sidereal Time (GMST) has the value [3.1], [3.6]:

$$\begin{aligned} \mathrm{GMST}\left(0^h\,\mathrm{UT1}\right) &= 24110^s.54841 + 8640184^s.812866 \cdot T_o \\ &\quad + 0^s.093104 \cdot T_o^2 - 0^s.0000062 \cdot T_o^3 \end{aligned} \tag{3.2}$$

For an arbitrary time of the day, the expression may be generalized to obtain the Greenwich hour angle GHA by multiplying this time with the factor 1.00273790935, adding this result to (3.2) and convert it into degrees (if so desired)

$$\mathrm{GMST}\ (\mathrm{UT1}) = 24110^s.54841 + 8640184^s.812866\mathrm{T_o} + 1.00273790935\mathrm{UT1} + 0^s.093104\mathrm{T}^2 - 0^s.0000062 \cdot T^3 \tag{3.3}$$

where T is the time in Julian centuries since the 1st of January 2000, 12 h, i.e. 2000 Jan. 1.5 :

$$\mathrm{T} = \frac{\mathrm{JD(UT1)} - 2451545}{36525} \tag{3.4}$$

and JD is the Julian Date.

Ecliptic and Earth equator at 2000 Jan 1.5 define the *J2000 system*.

The second and third order terms in (3.2) and (3.3) reflect the influence of the planets on the two body system Sun – Earth/Moon. They do not reflect planetary and lunar precession/nutation which influences the position of the vernal equinox in an inertial frame.

The most useful relation for computer software is one that uses only JD (UT1) (see [3.8 / 3.15]).

$$\begin{aligned} GMST(^\circ) &= 280.46061837 + 360.98564736629 \cdot \left(JD - 2451545.0\right) + \\ &\quad + 0.000387933T^2 - T^3 / 38710000 \end{aligned} \tag{3.5}$$

with T given by (3.4).

The difference between UT1 and TT or TAI (atomic clock time, to be explained below) can only be determined retrospectively. This difference is announced by the International Earth Rotation Service (IERS) and is handled in practice by the implementation of leap seconds (maximum of two in one year).

The above formulae contain implicitly the Earth's mean angular rotation $\omega_\oplus$ in degrees per second [3.15].

$$\omega_\oplus\left(rad/s\right) = \left\{1.002737909350795 + 5.9006 \cdot 10^{-11} T - 5.9 \cdot 10^{-15} T^2\right\} \cdot \frac{2\pi}{86400s} \tag{3.6}$$

3.1.5 Coordinated Universal Time (UTC)

Coordinated Universal Time (UTC) is obtained from atomic clocks running at the same rate as TT or TAI (chapters 3.1.6/7). The UTC time scale is always within 0.7 seconds of UT1. By the use of leap seconds, care is taken to ensure that this difference is never exceeded. However, because of the introduction of the leap seconds it becomes clear that this time scale is not steady.

The International Earth Rotation Service (IERS) can add leap seconds and is normally doing this at the end of June or December of each year if necessary. The actual UTC can only be determined for a previous point in time but predictions for the future are published by the IERS. This fact should be noted when future missions are planned on the base of the UTC time standard.

UTC can be obtained by the difference of the predicted value DUT1 or the past value ΔUT between UT1 and UTC published in the IERS Bulletin A (http://maia.usno.navy.mil/) which contains previous leap seconds and predictions [3.18] or in ftp://tycho.usno.navy.mil/pub/series:

$$\mathrm{UTC} = \mathrm{UT1} - \mathrm{DUT1} \quad \text{or} \quad \mathrm{UTC} = \mathrm{UT} - \Delta\mathrm{UT} \tag{3.7}$$

This relation is needed to obtain UT1 (UT) from UTC.

3.1.6 International Atomic Time (TAI)

TAI provides the practical realization of a uniform time scale based on atomic clocks. This time is measured at the surface of the Earth. Since this time scale is a steady one, it differs from UTC by an integral number of leap seconds introduced up the current point in time:

$$\mathrm{TAI} = \mathrm{UTC} + \mathrm{LS} \tag{3.8}$$

where LS is the number of leap seconds. The unit of TAI is the SI second.

TAI is made available every month in the BIPM “Circular T” at their web site in the following address: ftp://62.161.69.5/pub/tai/publication [3.20]

3.1.7 Terrestrial Dynamic Time (TT)

Terrestial Time (TT) – formerly Terrestrial Dynamical Time (TDT) - is to be understood as time measured on the geoid. It has conceptionally a uniform time scale. TT is the independent variable of *geocentric ephemerides*. TT replaced Ephemeris Time (ET) in 1984. The difference between TT and the atomic time scale (TAI) is a constant value of 32.184 seconds [3.1]:

$$\mathrm{TT} = \mathrm{TAI} + 32.184^{s} \tag{3.9}$$

One therefore obtains also the relationship:

$$\mathrm{UTC} = \mathrm{TT} - 32.184^{s} - \mathrm{LS} \tag{3.10}$$

TT does not take into account relativistic corrections. It is used as an independent argument of geocentric ephemeris.

3.1.8 Geocentric Coordinate Time (TCG)

Geocentric Coordinate Time TCG represents the time coordinate of a four dimensional reference system and differs from TT by a constant scale factor yielding the relation

$$TCG = TT + L_G \cdot (JD - 2443144.5) \cdot 86400\, s \tag{3.11}$$

$L_G = 6.9692903 * 10^{-10}$

For practical reasons this equation can also be put into the following relation :

$$\mathrm{TCG} = \mathrm{TT} + 2.2\ \mathrm{s/cy} * (\mathrm{year} - 1977.0) \tag{3.12}$$

cy = century

3.1.9 Barycentric Dynamic Time (TDB)

In a general relativistic framework, time is not an absolute quantity but depends on the location and motion of a clock. TDB refers to the center of mass of the solar system and is the independent variable of *barycentric planetary ephemerides*. Since the differences compared to TT are fairly small, the corrections can be determined by the following approximation [3.2]:

$$\mathrm{TDB} = \mathrm{TT} + 0.001658^{s} \cdot \sin \mathrm{g} + 0.000014^{s} \cdot \sin(2\mathrm{g}) \tag{3.13}$$

with g being the mean anomaly of the Earth in its orbit given by

$$\mathrm{g} = 357.53 + 0.9856003 \cdot \left(\mathrm{JD}(\mathrm{UT1}) - 2451545.0\right) \quad [\mathrm{deg}] \tag{3.14}$$

A more accurate formula can be found in [3.3], but since the differences to the results of the formula given above are smaller than 20 microseconds [3.2], it has been neglected in the RSS.

3.1.10 Barycentric Coordinate Time (TCB)

The Barycentric Coordinate Time TCB has been introduced to describe the motion of solar system objects in a non rotating relativistic frame centered at the solar system barycenter. TCB and TCG exhibit a rate difference which depends on the gravitational potential of the Sun at the mean Earth-Sun distance 1 AU and the Earth´s orbital velocity. The accumulated TCB-TT time difference amounts to roughly 11 s around epoch J2000 [3.1].

$$TCB = TCG + L_C \cdot (JD - 2443144.5) \cdot 86400\, s + P \tag{3.15}$$

(Mc Carthy 1996) and

$$\begin{aligned} P \approx {} & +0^s.0016568 \cdot \sin(35999°.37T + 357°.5) \\ & + 0^s.0000224 \cdot \sin(32964°.5T + 246°) \\ & + 0^s.0000138 \cdot \sin(71998°.7T + 355°) \\ & + 0^s.0000048 \cdot \sin(3034°.9T + 25°) \\ & + 0^s.0000047 \cdot \sin(34777°.3T + 230°) \\ T = {} & (JD - 2451545.0)/36525 \end{aligned} \tag{3.16}$$

L_c = 1.4808268457 10^{-8}

The largest contribution is given by the first term. When neglecting the other terms we can approximate P by:

$$P = 0.001658^{\,s} \sin(g) + 0.000014^{\,s} \sin(2g) \tag{3.17}$$

TCB as defined above (3.15) will, however, not be used in the VeRa simulation routines.

3.1.11 Dynamical Time Scale T_{eph} for the JPL DE 405 Ephemeris

During the years 1984 – 2003 the time scale of ephemerides referred to the barycenter of the solar system was TDB.

From 2004 onwards this time scale for the JPL DE 405 ephemeris will be replaced by T_{eph} [3.18].

T_{eph} is approximately equal to TDB, but not exactly. On the other hand, as will be shown, T_{eph} is mathematically and physically equivalent to the newly-defined TCB, differing from it by only an offset and a constant rate [3.19]. Within the accuracy required by VeRa we can use [3.18].

$$T_{eph} \sim \text{TDB} \tag{3.18}$$

3.1.12 Spacecraft Time (OBT)

The S/C has a clock driven by the onboard oscillator. All activities onboard are based on this clock and time for commands, attitude profiles are expressed in onboard time. Onboard time (OBT) has a coarse and a fine part (seconds and fractions of seconds). Many processes onboard are only accurate to coarse time. (For MEX certain mode transitions have delays of several seconds, e.g. from commanded time to executed time, actual attitude control may even have higher delays in slews due to the controller [3.5]).

In order to command activities to the S/C (which require onboard time) the ground performs time correlation. Time correlation is performed by the MCS. The basic elements are as follows: The S/C sends special packets (time packets) which contain an onboard time stamp. When the packets arrive at the G/S the packets are stamped with UTC time. FD provides the profile for the One Way Light Time (i.e. the time for transmission of the signal from the S/C to the ground station). The MCS subtracts to the UTC time stamp the One Way Light Time and any other known delays at the S/C or at the ground station. The MCS performs several such measurements, which provide a table of corresponding onboard times with UTC times. A linear fit is performed regularly. This is used then to translate UTC time to onboard time for generating commands, and onboard time to UTC for TM datation. [3.5].

We name this process which converts UTC in onboard time MCSFIT(UTC) and set

$$OBT = MCSFIT(UTC) \tag{3.19}$$

OBT becomes also relevant when the attitude dynamics of the S/C has to be reconstructed based on attitude sensor values digitized and stored in the S/C memory and transmitted to Earth via TM. Any onboard delay from the actual measurement to the onboard time mark must be known to the Radio Science Team for the purpose of later data analysis.

3.1.13 Light time corrections

The travel time of the radio signal from the instant of transmission to the instant of reception can not be neglected in interplanetary missions. An occultation at Venus will take place at an earlier time than as observed from Earth. Due to the finite velocity of light, the geometric relative positions of S/C, planet, and Earth at time of signal reception are different from those at the time of signal emission. These light time corrections can have durations up to 13 minutes (Venus) or 22 minutes (Mars), depending on the relative location of both the planet and the Earth. The light time correction is calculated iteratively starting from an initial value (assuming infinite speed of light).

All predictions and simulations for Doppler, ranging, occultation, and bistatic radar measurements must include this effect.

3.2 Time Basis Convention used for Radio Science Experiments

We described above the conversion of the TDB (T_{eph}) time basis used for predicting planetary ephemeris data into a time basis which is adjusted to mean solar time UTC.

If this time translation is done wrong the time stamp, given to the measurements at the G/S, is also wrong. That means the predictions for the observables will be false and the quality of the scientific results will suffer since the scientifically valuable information is gained by the extraction of predicted values from measured values.

Since VeRa comprises also of active attitude maneuvers of the S/C a further consequence would be that the maneuvers would be performed at the astrodynamically wrong time and could lead to erroneous results.

The selection of the proper time basis is determined by the scientific tasks to be performed. These are:

- Prediction of Doppler and ranging data for a specific time (UTC) at the G/S.
- Execution of an onboard command sequence (e.g. a specific attitude) at the required precise onboard time (OBT).
- Reconstruction of the attitude manoeuvres based on attitude sensor information stored as HK data onboard the S/C with OBT used as time mark.

The prediction of Doppler, ranging data and attitude maneuvers depends critically on the orbital dynamics of the S/C which again is dependent on the planetary ephemerides (see chapter 3.5). The planetary ephemeris are calculated by the JPL/DE405 program which assumes as inertial reference frame the J2000 reference frame. If desired this program also transforms an input state, in either direction, between barycentric and planetocentric system. The positions of the planets are given in a pure “geometric” sense, i.e. the speed of light is assumed to be infinite.

The time basis selected for the independent variable “time” is the Barycentric Dynamical Time TDB or T_{eph}, respectively. (The potential use of the Barycentric Coordinate Time TCB will not be discussed here). It is therefore required to match TDB (T_{eph}) time with UTC time in the prediction software routine. Light Travel Time and other known delays have to be considered additionally.

The onboard time (OBT) which controls the precise execution of the onboard commands depends again on the planetary ephemeris data and the orbit dynamics of the spacecraft. Hence, also here the software routines for programming the maneuvers must convert TDB/TCB into UTC and further into OBT.

Leap second and DUT 1 forecasts generated by the IERS are considered in the prediction and simulation software for the orbit phase.

- In order to predict the Doppler frequency shift and the ranging delay for a specific time (UTC) at the G/S, the relevant time instants for an occultation are calculated by the orbit module in RSS on the TDB time basis *including the effect of light time* for as well one

way as two way links. With the formulas given above, we then have to convert TDB into UTC according to:

$$UTC = UT\,1 - DUT\,1 = TDB - LS - 32.184^{s} - P \cong TDB - LS - 32.184^{s} - 0.001658^{s}\sin(g) \quad (3.19)$$

- In order to have an onboard command executed at the proper S/C time (OBT) as well as at the proper TDB time the S/C time has to be programmed such that:

$$OBT = MCSFIT(UTC) \quad (3.20)$$

3.3 Celestial and Terrestrial Reference Systems

In addition to the time basis effects discussed in chapters 3.1/2 we also have to consider the fact that the Earth-fixed reference system the *International Terrestrial Reference System (ITRS)* is not inertially fixed in space. The coordinates of a vector describing the position of a G/S in the geocentric ITRS frame must be transformed according to the motion of the Earth´s equatorial and orbital plane and its rotation axis to obtain the proper position and velocity vector of the G/S available for the prediction of Doppler and ranging data.

The inertially fixed reference system is called the *International Celestial Reference System* (ICRS), its fundamental plane is closely aligned with the mean equator at J2000. As mentioned above the planetary ephemeris data are given by JPL/DE405 in the J2000 reference system, therefore the actual Earth orientation (of date) must be transformed such that it is compatible with the J2000 reference system. In other words, the coordinates of a G/S vector **r** given in the ITRS frame must be transformed into the ICRS (J2000) frame.

3.3.1 Coordinate Changes Due to Precession

The presence of other solar system bodies results in small secular variation of the orbital pane of the Earth known as *planetary precession*. At the same time the Earth´s axis of rotation is perturbed by the torque exerted on the equatorial bulge by the Sun and Moon known as *lunisolar precession*. The combined effect of precession on the orientation of the ecliptic and the equator are illustrated in **Fig. 3.3-1** where the motion of both planes is described with respect to the mean equator and ecliptic of the reference epoch J2000 (2000 January 1.5).

The system defined by the mean equator and equinox of J2000 is called the *International Celestial Reference System* (ICRS).

We obtain for the combined precession p in longitude [3.1]

$$p = \Lambda - \Pi = 5029''.0966 \cdot T + 1''.11113 \cdot T^2 - 0''.000006T^3 \quad (3.21)$$

which shows us that in the year 2006 we have to consider an effect of approx. 0.08 ° equivalent to a potential time delay of approximately 20 seconds w.r.t. the year 2000!

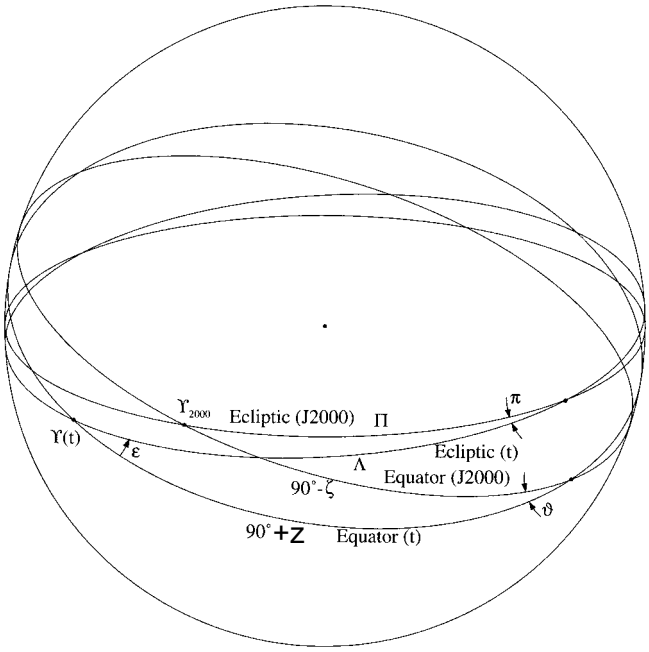

Fig. 3.3-1: The effects of precession on the ecliptic, equator and vernal equinox [after 3.1]

According to **Fig. 3.3-1** the transformation from coordinates of a vector $\mathbf{r}_{ICRS}$ (referred to the mean equator and equinox of J2000) to coordinates referred to the mean equator and equinox of some other epoch may be written as [3.1] :

$$\mathbf{r}_{mod} = \mathbf{P}\ \mathbf{r}_{ICRS} \qquad (3.22)$$

Where the matrix **P** and the matrix elements p_{ij} are given in [3.1] by the equations (5.46) and (5.47).

3.3.2 Coordinate Changes due to Nutation.

Aside from the secular precessional motion the orientation of the Earth´s rotation axis is affected by small periodic perturbations that are known as nutation. They are due to the monthly and annual variations of the lunar and solar torque.

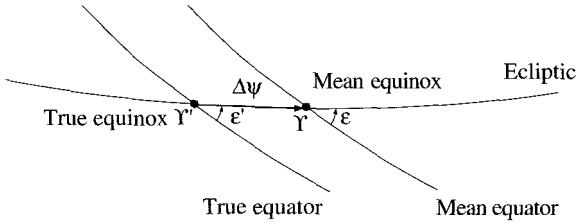

Fig. 3.3-2: The shift in the position of the equator, the ecliptic and the vernal equinox, caused by nutation [3.1]

The transformation from mean-of-date coordinates (referred to the mean equator and equinox) to true-of-date coordinates (referred to the true equator and equinox) may be written as

$$\mathbf{r}_{tod} = \mathbf{N}(T)\,\mathbf{r}_{mod} \qquad (3.23)$$

Time T is given by

$$T = (JD(TT) - 2451545.0)/36525 \qquad (3.24)$$

The matrix elements n_{ij} are given in [3.1]

Combining equations (3.19) and (3.20) we obtain

$$\mathbf{r}_{tod} = \mathbf{N}\,\mathbf{P}\,\mathbf{r}_{ICRS} \qquad (3.25)$$

It shall be mentioned that the above transformations describe the motion of the Earth as a rigid body in space and relate UTC to the *mean equinox* (epoch 2000) via equation (3.2/3). If we want to include the *true equinox* instead we have to consider the fact that the true Earth rotation angle differs by $\Delta\psi \cos\varepsilon$ (see **Fig. 3.3-2**). This effect is treated in the next chapter.

3.3.3 Rotation about the Celestial Ephemeris Pole

The IAU precession and nutation theories yield the instantaneous orientation of the Earth´s rotation axis, or more precisely, the orientation of the *Celestial Ephemeris Pole* (CEP) with respect to the International Celestial Reference System (ICRF). The Celestial Ephemeris Pole (CEP) differs slightly from the instantaneous rotation axis. The adoption of the CEP is related to the fact that the rotation axis performs a predictable daily motion around the CEP under the action of the Sun and Moon and is not, therefore, a proper reference pole for theoretical and observational reasons.

The rotation about the CEP axis itself is described by the Greenwich Mean Sidereal Time (GMST) that measures the angle between the mean vernal equinox and the Greenwich Meridian. Given the UT1-UTC or UT1-TAI time difference as monitored and published by the IERS, the Greenwich Mean Sidereal Time at any instant can be computed from the relation (3.3).

Similar to GMST, the Greenwich Apparent Sidereal Time (GAST) measures the hour angle of the *true equinox*. Both values differ by the nutation in right ascension

$$\text{GAST-GMST} = \Delta\psi \cos\varepsilon \tag{3.26}$$

Which is also known as the *equation of equinoxes.*

(If we express $\Delta\psi$ in arcseconds the correction in time seconds is $\Delta\psi \cos\varepsilon$ / 15).

With sufficient accuracy we can use the following expressions for ε and $\Delta\psi$ [3.1]:

$$\varepsilon \quad = 23°.43929111 - 46.''8150\ T - 0.''00059\ T^2 + 0.''001813\ T^3 \tag{3.27}$$

$$\Delta\psi \quad = -17.''200 \sin(\Omega) \tag{3.28}$$

With Ω given by:

$$\Omega = 125°02'40.''280 - 1934°08'10.''539\ T + 7.''455\ T^2 + 0.''008\ T^3 \tag{3.29}$$

and T given by (3.4).

For calendar year 2006 the correction GAST – GMST amounts to approximately 2.4´´ corresponding to a time correction of ~ 0.17 seconds.

Given the apparent sidereal time, the matrix

$$\mathbf{\Theta}(t) = \mathbf{R}_Z(GAST) \tag{3.30}$$

yields the transformation between the true-of-date coordinate system and a system aligned with the Earth equator and Greenwich meridian.

3.3.4 Transformation to the International Reference Pole

The system which is used to describe globally and geodetically the Earth´s surface is the *International Terrestrial Reference Frame* (ITRF). Because of internal motions and shape deformations of the Earth, an axis defined by the locations of a set of observatories on the surface of the Earth is not fixed with respect to the rotation axis that defines the celestial pole. The movement of one axis with respect to the other is called *polar motion* [3.20]. The Earth's instantaneous spin axis traces a quasicircular, quasiperiodic path approximately 20 m in diameter.

The transformation from true-of-date coordinates (as defined by the theory of precession and nutation) to the body-fixed *International Terrestrial Reference System (*ITRS) is given by [3.1]

$$\mathbf{r}_{ITRF} = \mathbf{\Pi}(t)\mathbf{\Theta}(t)\mathbf{r}_{tod} \tag{3.31}$$

Here $\mathbf{\Theta}$ describes the Earth´s rotation about the CEP axis, while Π accounts for polar motion.

In order to compute the transformation from the *International Celestial Reference System* (ICRS) – or the mean equator and equinox of J2000 to the *International Terrestrial Reference System* (or the reference pole and Greenwich meridian) for a different epoch we have to apply step-by-step transformation matrices for precession (**P**), nutation (**N**), Earth rotation $\mathbf{\Theta}$, and polar motion Π which yields

$$\mathbf{r}_{ITRS} = \mathbf{U}\,\mathbf{r}_{ICRS} = \Pi\,\mathbf{\Theta}\,\mathbf{N}\,\mathbf{P}\,\mathbf{r}_{ICRS} \tag{3.32}$$

The matrix Π is given by

$$\mathbf{\Pi} \approx \begin{pmatrix} 1 & 0 & +x_p \\ 0 & 1 & -y_p \\ -x_p & +y_p & 1 \end{pmatrix} \tag{3.33}$$

x_p, y_p are shown in Fig. 3.3-3. Their values are in the range of 10^{-6} to 10^{-7} rad [3.1, p.190]. They are published in the IERS Bulletin B. The polar motion predictions are published in the IERS Bulletin A (http://maia.usno.navy.mil/).

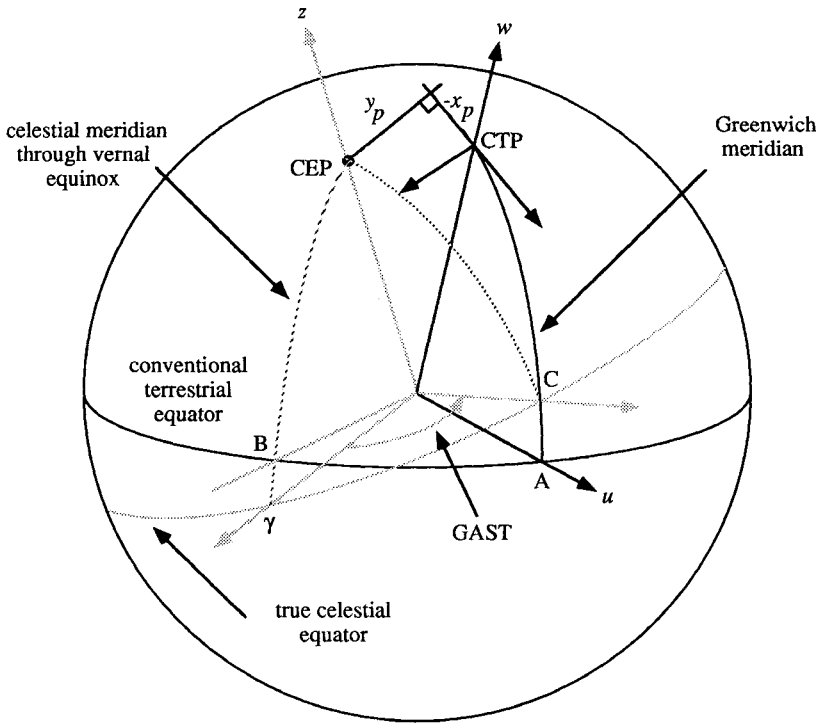

Fig. 3.3-3: Conventional terrestrial system. To avoid time-dependent positions of earth stations, the CTRS is referenced to the CTP and the Greenwich meridian [7.1]. CEP= Celestial Ephemeris Pole. CTP=Conventional Terrestrial Pole ($\perp$ to conventional terrestrial equator)

The contribution of the polar motion Π results in rotation angles of ~ 0.´´3 equivalent to time errors of ~0.02 seconds.

3.3.5 Earth Ellipsoid - Ground Station Coordinates

Knowing the exact position of the ground station on Earth is crucial for the prediction of an occultation event. The WGS-84 system is used as a reference ellipsoid for the Earth to define the coordinates. Ref. [3.1] gives an equation to compute cartesian coordinates if the geodetic (= geocentric) longitude λ, the geodetic latitude φ and altitude h above the reference ellipsoid with a radius R_{ref} and a flattening f are given:

$$r = \begin{pmatrix} (N+h)\cos\varphi\cos\lambda \\ (N+h)\cos\varphi\sin\lambda \\ \left((1-f)^2\ N+h\right)\sin\varphi \end{pmatrix} \tag{3.34}$$

where

$$N = \frac{R_{ref}}{\sqrt{1-f\left(2-f\right)\sin^2\varphi}} \tag{3.35}$$

and 1/f = 298.257223563 [3.1]

The motion of a ground station in an inertial reference system is dominated by the Earth rotation with a velocity of 460 m/s at the equator and the translatory motion of the Earth around the solar system barycenter (~ 30 km/s). When the motion of the ground station is modeled in the inertial *International Celestial Reference System* ICRS, the position $\mathbf{r}_{\text{ITRS}}$ of the station in the *International Terrestrial Reference System* (ITRS) has to be transformed using the matrices derived above leading to

$$\mathbf{r}_{\text{ICRS}} = \mathbf{U}^T(t)\mathbf{r}_{ITRS} = \mathbf{P}^{\text{T}}(t)\,\mathbf{N}^{\text{T}}(t)\,\boldsymbol{\Theta}^{\text{T}}(t)\ \boldsymbol{\Pi}^{\text{T}}(t)\ \mathbf{r}_{\text{ITRS}} \tag{3.36}$$

In addition, the precise computation of the position of the ground station requires modeling site displacements due to tidal perturbations and plate motion. These effects will, however, not be considered here at this time (regard also the comments made about $\boldsymbol{\Pi}$ in chapter 3.3.4).

3.3.6 The Velocity of a G/S in the Inertial International Reference System ICRS

If we adopt the geocentric ICRS, then the velocity $\mathbf{V}_{\text{ICRS}}$ of the G/S is approximated by the following expression

$$\mathbf{v}_{ICRS} = \frac{d}{dt}\mathbf{r}_{ICRS} \sim \mathbf{P}^T(t)\mathbf{N}^T(t)\frac{d\boldsymbol{\Theta}^T(t)}{dt}\boldsymbol{\Pi}^T(t)\mathbf{r}_{ITRS} \tag{3.37}$$

Here we have neglected the slow variations of $\mathbf{P}, \mathbf{N}, \text{and } \boldsymbol{\Pi}$

Further, from (3.30)

$$\boldsymbol{\Theta}^T(t) = \mathbf{R}_z\left(-GAST\right) = \mathbf{R}_z\left(-\Delta\psi\cos\varepsilon - GMST\right) \tag{3.38}$$

and

$$\boldsymbol{\Theta}^T(t) = \begin{pmatrix} \cos(GAST) & -\sin(GAST) & 0 \\ \sin(GAST) & \cos(GAST) & 0 \\ 0 & 0 & 1 \end{pmatrix} \tag{3.39}$$

$$\frac{d\boldsymbol{\Theta}^T(t)}{dt} = \frac{d(GAST)}{dt} \begin{pmatrix} -\sin(GAST) & -\cos(GAST) & 0 \\ \cos(GAST) & -\sin(GAST) & 0 \\ 0 & 0 & 0 \end{pmatrix} \tag{3.40}$$

with the definition

$$\frac{d(GAST)}{dt} = \omega_{\oplus} \tag{3.41}$$

Equation (3.40) can also be written as

$$\frac{d\boldsymbol{\Theta}^T(t)}{dt} = \omega_{\oplus} \begin{pmatrix} 0 & -1 & 0 \\ 1 & 0 & 0 \\ 0 & 0 & 0 \end{pmatrix} \boldsymbol{\Theta}^T(t) \tag{3.42}$$

We then derive for the velocity of a G/S in the geocentric ICRS

$$\mathbf{v}_{ICRS} = \omega_{\oplus}\, \mathbf{P}^T(t)\mathbf{N}^T(t) \begin{pmatrix} 0 & -1 & 0 \\ 1 & 0 & 0 \\ 0 & 0 & 0 \end{pmatrix} \boldsymbol{\Theta}^T(t)\boldsymbol{\Pi}^T(t)\mathbf{r}_{ITRS} \tag{3.43}$$

For $\omega_{\oplus}$ we set (see equation 3.6)

$$\omega_{\oplus}(rad/s) = 1.002737909351 \cdot \frac{2\pi}{86400s} \tag{3.44}$$

3.3.7 Venus and Mars Ellipsoids

Venus has a spherical shape with an equatorial radius and polar radius of 6051.8 km. For Mars we assume a rotational symmetric ellipsoid. The polar and equatorial semi-major axis have a length of 3376.20 km and 3396.19 km, respectively [3.13].

3.4 Planetary Ephemeris and Planetary Coodinates

The position of the planets are calculated using the JPL/DE405 ephemeris model. The ephemeris data are given in the barycentric time basis TDB and in either the heliocentric or the geocentric J2000 system in a pure geometrical sense, i.e. assuming infinite speed of light. After implementation of light time effects, the RSS routines will calculate for an observer located at a specific G/S the occultation scenario, HGA attitude manoeuvers, Doppler and ranging data predictions. All timing data, however, still have to be converted from TDB to UTC according to equation (3.16) or (3.17), respectively, to make them suited for G/S observations and predictions.

All rotational elements and planetary coordinates necessary to describe the VEX S/C orbit around Venus are taken from Seidelmann et al. [3.17].

3.5 Aberration

Aberration effects are not treated in our analysis since the Radio Science measurements are not concerned with the “optical” position of the S/C. (The beam width of the antennas is large in comparison to the aberration effect). The contribution of the aberration effect to the Doppler and group delay observables is considered to be below the sensitivity threshold of the VeRa measurements.

3.6 Occultation Scenario

The occultation scenario as seen from Venus (not considering ray bending effects) is sketched in Fig. 3.5-1

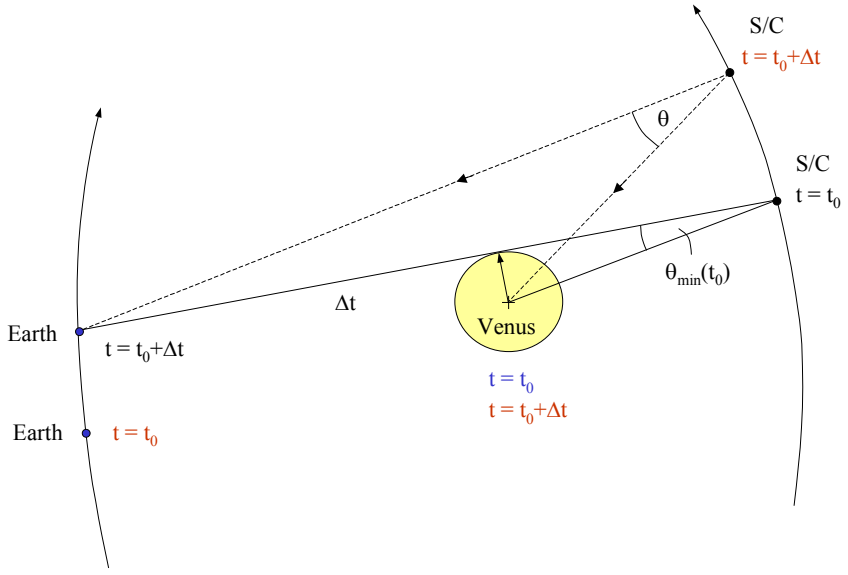

Fig. 3.5-1: Planetary occultation scenario as seen from Venus (ray bending effects not considered). Time basis is TDB.

For our purposes, we assume that the light travel time S/C – Venus is negligible in comparison to the light travel time S/C – Earth. The criteria for an occultation is then given when the angle theta reaches a minimum value at the time t_o. The radio signal, however, reaches the Earth at some later time $t_o + \Delta t$.

Since the time basis used for mission planning and control is UTC it is necessary to convert the time for the occultation events when recorded at the G/S from TDB to UTC.

4. MODELING OF VENUS ATMOSPHERE

4.1 Introduction

A planetary atmosphere of neutral gas molecules and atoms exhibits both refractive and absorptive radio effects. In the following we will focus on the refractive effects only.

The region of the neutral atmosphere of Venus extends to a height of approximately 100 km where the neutral gas becomes ionised. The region of the ionosphere reaches to altitudes of approximately 250 km and its structure depends strongly on local time and coupling effects to the solar wind plasma.

The propagation of microwave rays in the Venusian environment can be calculated very accurately with analytical approximations for the altitude dependence of atmospheric and ionospheric refractivity. The method which will be applied is the *ray tracing technique*. In the following we will consider a spherically symmetric atmosphere.

4.2 Basic Relationships

The refraction index n of a molecular atmosphere is given by the product density times "refractive volume" for a molecule (~ magnitude of the classical volume of a molecule) [4.5]. The knowledge of n as a function of height allows one to therefore derive an atmospheric density profile and to draw further conclusions about temperature, pressure and chemical composition in the atmosphere. For Venus a model atmospheric height profile for n was determined based on the radio science instrument data gained with the Magellan spacecraft [4.1].

First, the gradient of n as a function of altitude h was calculated by numerical differentiation of n(h) (blue line). The data were then fitted and approximated according to an e-folding law (red line shown in **Fig. 4-1**):

$$\frac{dn}{dh} \approx e^{-(az^3+bz^2+cz)} \tag{4.6}$$

with $z = (h_0 - h)/H$, H being a scale height

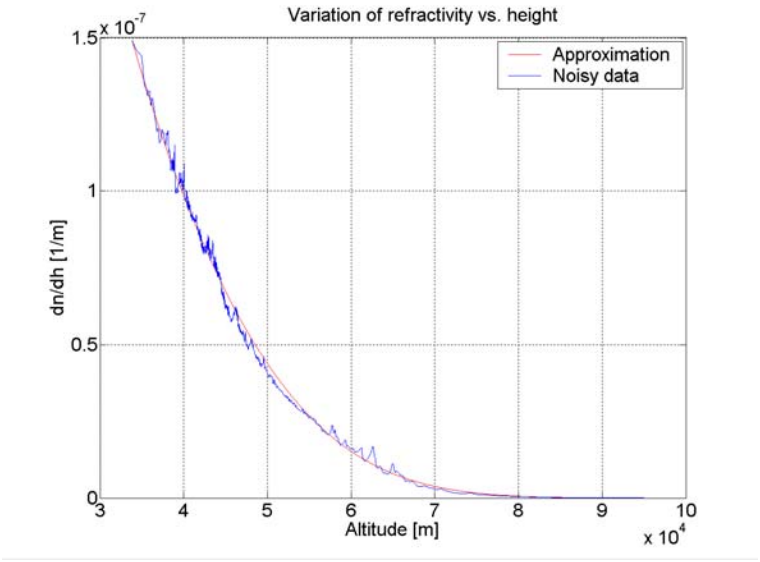

Figure 4-1: Gradient of index of refraction vs. height. Instrumental and numerical noise was smoothed by red curve [4.6]

The ionospheric electron density profile obtained from the Mariner 5 [4.2] and 10 Mission [4.2] is shown in **Fig. 4.-2**. It shows – as expected - an extreme variability with local time.

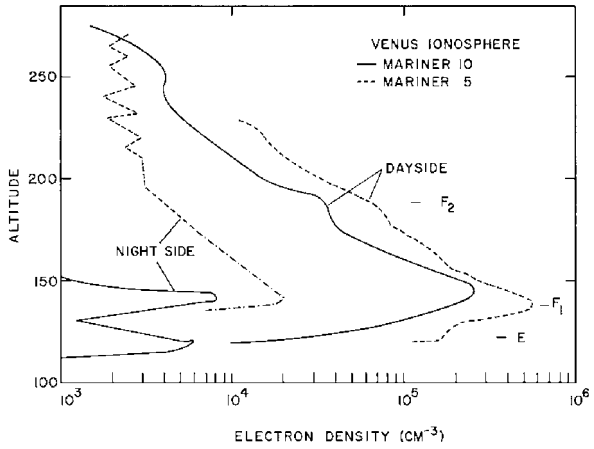

Fig. 4-2: Day- and nightside ionospheric density profiles (ref: B.M. McCormac, Atmospheres of Earth and the Planets, D. Reidel Publishing Company, 1975)

A Chapman profile is applied to describe the density vs. altitude profile of an ionosphere [4.7]

$$n = n_0 e^{1-y-\frac{1}{\cos\xi}e^{-y}} \tag{4.7}$$

$$y = \frac{h_0 - h}{H}$$

$$\begin{aligned} \xi &= && \text{angle between zenit and sun direction} \\ h_0 &= && \text{for } \xi\text{=0 height of maximum} \\ H &= && \text{scale height} \end{aligned} \tag{4.8}$$

In the RSS, the ionospheric dayside density profile can be numerically modelled with up to three superimposed Chapman profiles in order to allow a structuring of the ionospheric layer as shown in **Fig. 4-3**.

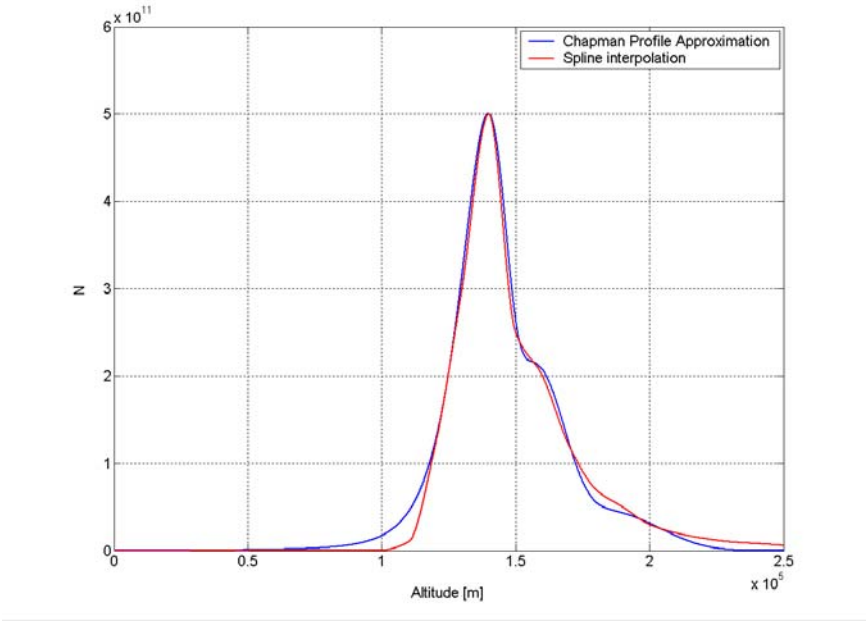

Fig. 4-3: Density profile of the Venus ionosphere interpolated with cubic splines and 3 superimposed Chapman profiles

5. RAY TRACING TECHNIQUE

5.1 Introduction

For computing the ray path through a dense planetary atmosphere, the following assumptions are made:

- given refractivity for all heights.
- spherically symmetric atmospheric density distribution
- given frequency of the rf signal (applicable for the ionospheric part only)

For the numerical calculations the Venus atmosphere model was composed of a large number of concentric spherical shells each with a constant refractivity and thickness ($\geq$1 m). The maximum altitude of the atmosphere was extended up to 250 km. In this picture, the geometric details of a ray path depend only on the entrance (exit) angle τ^* of the ray into the outermost layer of the atmosphere (**Fig. 5-1**). Each angle τ^* corresponds to a minimum scanned altitude r_0. Because of the inherent symmetry of the problem only one half of the total path needs to be numerically determined.

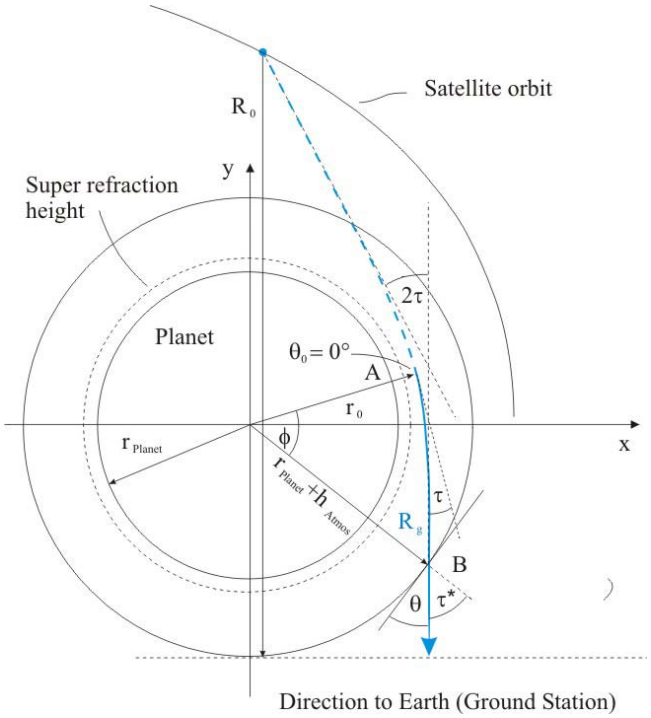

Fig. 5-1: Configuration between satellite, Venus atmosphere and ground station for occultation measurements. The total refraction angle of a ray equals 2τ

Figs. **5-2** show details of the ray tracing geometry. The spherically symmetric atmosphere was divided into concentric shells with a thickness of 1m each.

For spherical layers it can be shown that

$$n_0\, r_0 \sin\alpha_0 = n_i\, r_i \sin\alpha_i^* = const. \tag{5.1}$$

Further

$$\tan(\alpha) = \frac{(r+dr)\,d\varphi}{dr} \qquad \text{or} \qquad d\varphi = \frac{\sin(\alpha)}{\sqrt{1-\sin^2(\alpha)}} \cdot \frac{dr}{r} \tag{5.2}$$

We obtain with (5.1)

$$\varphi = \int_{r_1}^{r_2} \frac{const.}{\sqrt{r^2\, n^2 - const.^2}} \cdot \frac{dr}{r} \tag{5.3}$$

The angle θ results from (5.1) and α = 90°- θ

$$\theta = \arccos\left(\frac{n_0\, r_0}{n_i\, r_i}\cos\theta_0\right) \tag{5.4}$$

The geometrical length of the ray path (straight line approximation) in one spherical layer is

$$\Delta R_{gi} = \left\{(r_{i+1} - r_i)^2 + 2\left[1 - \cos(\phi_{i+1} - \phi_i)\, r_{i+1}\, r_i\right]\right\}^{\frac{1}{2}} \tag{5.5}$$

The sum over all concentric shells is

$$R_g = \sum_i \Delta R_{gi} \tag{5.6}$$

resulting in an optical path length of (for definition see 2.3.1)

$$R_{opt} = \sum_i n_i\, \Delta R_{gi} \tag{5.7}$$

In order to obtain the total refraction angle τ (see Fig. 5-1) the increments $\Delta\tau$ describing the refraction occurring at the transition from layer i into layer i+1 have to be integrated. The value $\Delta\tau$ is given by

$$\Delta\tau = \frac{\Delta n}{\bar{n}} \cdot 10^{-6} \operatorname{cotg}\bar{\theta} \tag{5.8}$$

$\overline{n}$ being the average of n_i and n_{i+1}. The bending angle $\overline{\theta}$ is the average of the bending angles generated between layer i and layer i+1 (see **Fig. 5-2**). It is now possible to calculate atmospheric ray paths for given minimum penetration altitudes r_0 (see **Fig. 2.4-1**). A library was generated containing a large number of ray paths (250.000) covering r_0 values from 32 km (height of super refraction) up to 240 km.

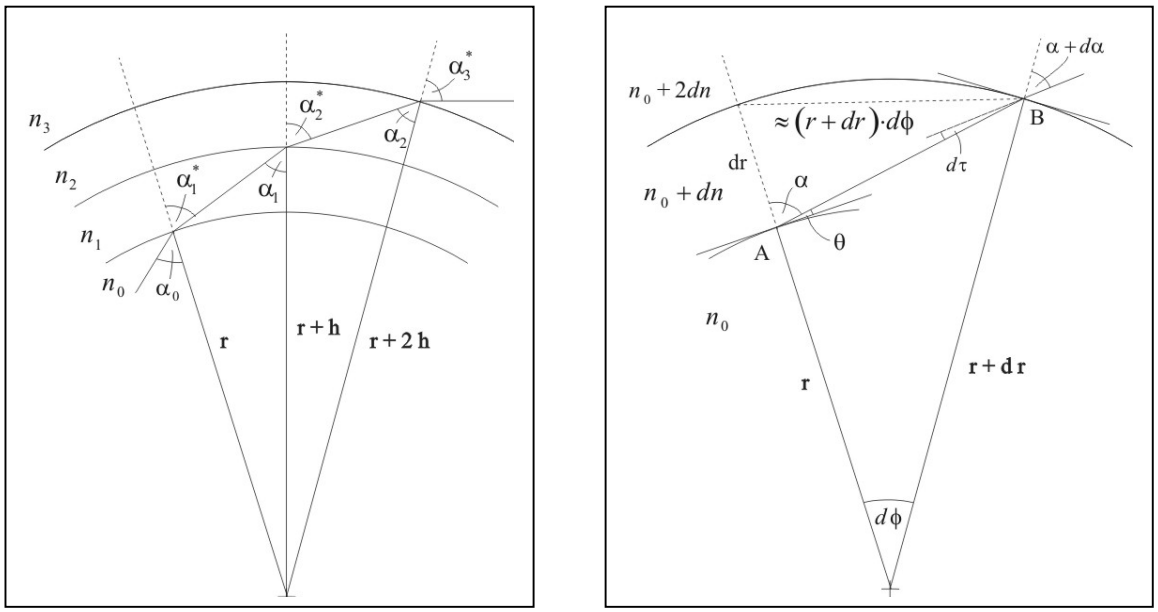

Fig. 5-2: a. Ray bending in spherical symmetric layers. b. Ray tracing geometry

Ray paths from the satellite to Earth will be calculated for every satellite position during an occultation phase. For that purpose we define an instantaneous plane containing the Earth (G/S), the centre of Venus and the satellite. A specially developed algorithm finds the particular ray which “connects” S/C and G/S.

Fig.5-3a and **Fig.5-3b** show for one example the points where a microwave ray emitted continuously from the S/C penetrates the Venus atmosphere. The satellite orbit is polar and centre of Venus, Earth and satellite are contained in nearly in one plane. Both illustrations (same occultation event– different projections) demonstrate the S/C attitude dynamics necessary to make a ray reception at the Earth´s G/S possible (and vice versa). It is obvious that the pointing manoeuvre required for the satellite will be different for each occultation. Naturally, the accuracy of the pointing manoeuver must be considerably better than the 3dB beam width of the HGA lobe.

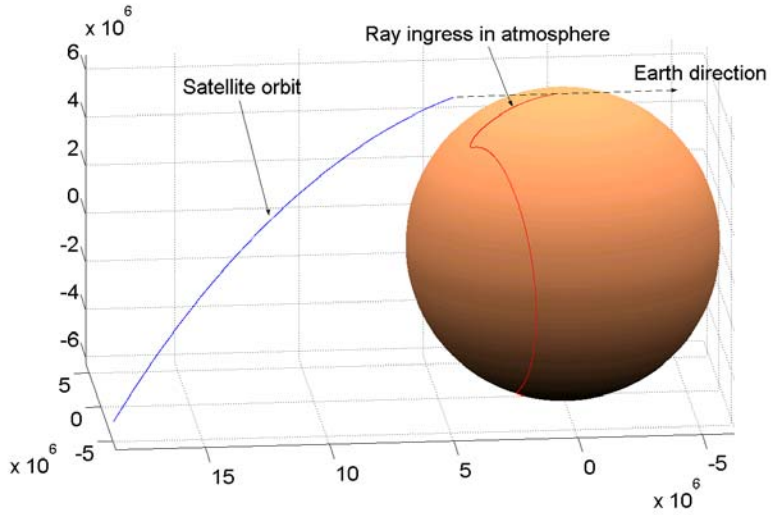

Fig. 5-3 a: View a: Part of the satellite orbit during an occultation (blue line) and the track of penetration points of the microwave ray into the atmosphere (red line), indicating the HGA pointing manoeuvre necessary to direct the radio beam to the G/S. Coordinate dimensions are in m.

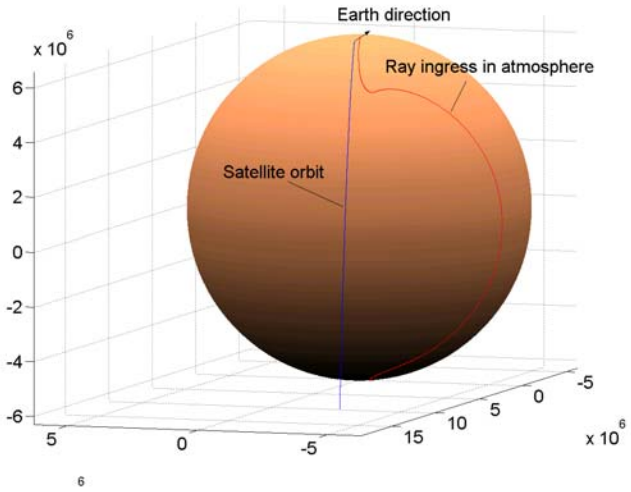

Fig. 5-3 b: View b: Same occultation as above, however, different projection.

6. ATTITUDE MANOEUVERS

6.1 Introduction

The following analysis will focus on the attitude dynamics of the S/C and its HGA which become necessary to compensate for ray bending effects in the Venusian atmosphere. We assume that the positions of Earth $\vec{\rho}$ and spacecraft $\vec{r}$ are given in a J2000 planetocentric equatorial coordinate system. The direction of the antenna is determined using the data file already defined in chapter 5. This data file contains for about 250 000 rays described by the values (x, y, τ), where (x, y) are the coordinates of the leaving ray from the Venus atmosphere in a 2-dimensional coordinate system and τ is the angle against the *y*-direction (τ^* in **Fig. 5-1**). The 2-dimensional frame is defined by the instantaneous co-planarity of Earth, centre of Venus and satellite. The direction to Earth is always assumed to be along the –y axis.

Due to the orbital dynamics involved the 2-dimensional frame must be newly defined for each incremental time step. For this purpose we introduce first a coordinate system with the unit vectors $(\vec{i}, \vec{j}, \vec{k})$ (see **Fig. 6-1**)

$$\vec{j} = -\frac{\vec{\rho}}{|\vec{\rho}|}\ ,\ \vec{k} = \frac{\vec{\rho}\times\vec{r}}{|\vec{\rho}\times\vec{r}|} \text{ and } \vec{i} = \vec{j}\times\vec{k}\ , \tag{6.1}$$

and perform the following task:

Find for a given satellite position at a specific instant the specific ray which approaches closest the Earth. In other words, we have to find one ray out of 250.000 rays meeting this criteria.

Each ray contained in the library is now rotated around the origin of the coordinate system such that it has a direction parallel to $-\vec{j}$ when it leaves the atmosphere at Q.

All rays are now traced “backwards” into the direction of the S/C. The one ray which has minimum distance to the S/C is now identified as the ray defining the pointing direction $\vec{e}_{antenna}(t)$ of the HGA.

The mathematical procedure applied is as follows:

The point *Q* (*x, y*) , where the ray is penetrating the atmosphere at egress, is described by the vector

$$\vec{b} = x\,\vec{i} + y\,\vec{j}$$

(note that $y < 0$ in the given data file).

The vector pointing from *Q* to earth is then given by

$$\vec{q} = \vec{\rho} - \vec{b} \, .$$

The ray rotation ξ is the angle between the unit vectors $\vec{e}_q = \vec{q} / |\vec{q}|$ and $\vec{e} = \sin\tau \, \vec{i} - \cos\tau \, \vec{j}$. $\vec{e}$ is the unit vector describing the direction of the ray leaving the atmosphere at Q. It should be noted that $\xi \approx \tau$ because the distance of Q from the earth is very large ($|\vec{q}| > 0.28\,AU$ and therefore $|\xi - \tau| < 0.01°$). We therefore can use τ instead of ξ to describe the rotation of the ray without an appreciable loss of accuracy.

All rays which enter the atmosphere of Venus at some point Q, described by $\vec{b}^* = x\,\vec{i} - y\,\vec{j}$ are now rotated by the same angle ξ . This procedure transforms Q into Q*. Q* being described by the vector $\vec{b}^{*\prime}$. This rotation is mathematically formulated as a quaternion $\tilde{q}$.

$$\tilde{q} = \cos\frac{\xi}{2} + \vec{k}\sin\frac{\xi}{2} \tag{6.2}$$

i.e. $$\vec{b}^{*\prime} = \tilde{q}(\vec{b}^*)\tilde{q}^{-1} \text{ and } \vec{e}^{*\prime} = \tilde{q}(\vec{e}^*)\tilde{q}^{-1} \tag{6.3}$$

The direction of the HGA is given by the vector $\vec{e}_{antenna}$.

$\vec{e}_{antenna}$ is found by picking the one (rotated) ray which has the minimal distance to the spacecraft, i.e. which fulfils the relation

$$\delta_{\min} = \min\left\{\arccos(\vec{e}^{*\prime} \cdot \vec{e}_q^{\,*\prime})\right\} \tag{6.4}$$

defining the boresight direction of the antenna

$$\vec{e}_{antenna} = -\vec{e}^{*\prime}_{\min} \tag{6.5}$$

where $\vec{e}_q^{\,*\prime} = \dfrac{\vec{r} - \vec{b}^{*\prime}}{|\vec{r} - \vec{b}^{*\prime}|}$ is the unit vector pointing from Q*' to the S/C.

6.2. Determination of Quaternions and Angular Rates

At the beginning of occultation $t = t_0$ we define our inertial coordinate system S_I by

$$\vec{E}_1 = \frac{\vec{\rho}}{|\vec{\rho}|} \text{ at } t = t_0, \; \vec{E}_2 = \frac{\vec{E}_1 \times \vec{e}_{Sun}}{|\vec{E}_1 \times \vec{e}_{Sun}|} \text{ at } t = t_0 \text{ and } \vec{E}_3 = \vec{E}_1 \times \vec{E}_2 \tag{6.6}$$

where the unit vector $\vec{e}_{Sun}$ gives the direction to the sun **(Fig. 6-2**), and $t = t_0$ defines the begin of an occultation. All times are TDB. The orbital motion of the Earth during the light travel time was neglected for the purpose of this study.

For each time step *t*, the pointing direction of the antenna is computed by the procedure given above and represented by the vector $\vec{e}_{antenna,P}(t)$ given in the planetocentric coordinate system S_P.

The vector $\vec{e}_{antenna,P}(t)$ has to be transformated into the reference coordinate system S_I, i.e.

$$\vec{e}_{antenna,\,I}(t) = \mathbf{R}\,\vec{\mathrm{e}}_{antenna,\,P}(t) \tag{6.7}$$

where $\mathbf{R}$ is the transformation matrix from S_P into $S_I = \{\vec{E}_1, \vec{E}_2, \vec{E}_3\}$.

At time $t = t_0$, i.e. beginning of occultation, the HGA points to the Earth and we have

$$\vec{e}_{HGA} = \vec{e}_{antenna}(t_0) = \vec{E}_1 \text{ at time } t = t_0 \tag{6.8}$$

as a unit vector describing the direction of the HGA at beginning of occultation.

At time $t > t_0$ the demanded direction of the antenna $\vec{e}_{antenna}(t)$ deviates from $\vec{E}_1$ and therefore $\vec{e}_{HGA}$ has to be rotated into $\vec{e}_{antenna}(t)$, which can be mathematically described by the quaternion $\tilde{q}(t)$, i.e.

$$\vec{e}_{antenna}(t) = \tilde{q}(t)\vec{E}_1\tilde{q}^{-1}(t) \tag{6.9}$$

The angular rates in the inertial frame follow from $\dot{\tilde{q}} = \frac{1}{2}\tilde{\omega}_I\,\tilde{q}$. We have

$$\tilde{\omega}_I = 2\,\dot{\tilde{q}}\,\tilde{q}^{-1} \tag{6.10}$$

where $\tilde{\omega}_I$ is the associated quaternion to the vector of angular velocity $\vec{\omega}_I$ given in the inertial frame S_I. The derivation of the quaternion $\dot{\tilde{q}}$ is described in the next subsection.

In a body frame $S_{BI} = \{\vec{e}_1, \vec{e}_2, \vec{e}_3\}$, which coincides with the reference frame S_I at beginning of occultation, i.e. at time t_0, the rates or angular velocities are represented by

$$\tilde{\omega}_{BI} = \tilde{q}^{-1}\tilde{\omega}_I\,\tilde{q} \tag{6.11}$$

In an arbitrary given body frame $S_B = \{\vec{e}_x, \vec{e}_y, \vec{e}_z\}$ the vector of angular velocity follows from

$$\tilde{\omega}_B = \mathbf{R}_B\tilde{\omega}_{BI} \tag{6.12}$$

where $\mathbf{R}_B$ is the transformation matrix from S_{BI} into S_B, i.e.

$$\begin{pmatrix} \vec{e}_x \\ \vec{e}_y \\ \vec{e}_z \end{pmatrix} = \mathbf{R}_B \begin{pmatrix} \vec{e}_1 \\ \vec{e}_2 \\ \vec{e}_3 \end{pmatrix} \tag{6.13}$$

6.3 Numerical Approximation

The components $q_k(t)$ (k = 1, 2, 3, 4) of a quaternion $\tilde{q}$ are approximated by Chebyshev polynomials, i.e.

$$q_k = \sum_{j=0}^{N-1} c_j^{(k)} T_j\left(\frac{2t - t_b - t_a}{t_b - t_a}\right) - \frac{1}{2} c_0 \text{ for } t_a \le t \le t_b \text{ and } k = 1, 2, 3, 4, \tag{6.14}$$

where t_a is the beginning of occultation and t_b the end of occultation. The Chebyshev coefficients $c_j^{(k)}$ are computed from the given exact components of the quaternion $\tilde{q}$ at the time marks t_i (i = 1, 2, ..., n). It should be noted that this time marks do not coincide with those required for the computation of the $c_j^{(k)}$. Therefore, an interpolation becomes necessary where we have used splines available in the MatLab Tool Box. However, linear interpolation would be also adequate.

For the angular rates we need $\dot{\tilde{q}}$, which follows from the approximated time derivatives $\frac{dq_k}{dt}$ of the components of the quaternion $\tilde{q}$ using the derivatives of the Chebyshev polynomials, i.e.

$$\frac{d}{dx} T_j(x) = \frac{j}{1 - x^2}\left(x T_j(x) - T_{j+1}(x)\right) \tag{6.15}$$

where

$$x = \frac{2t - t_a - t_b}{t_b - t_a} \quad \text{and} \quad \frac{dx}{dt} = \frac{2}{t_b - t_a} \tag{6.16}$$

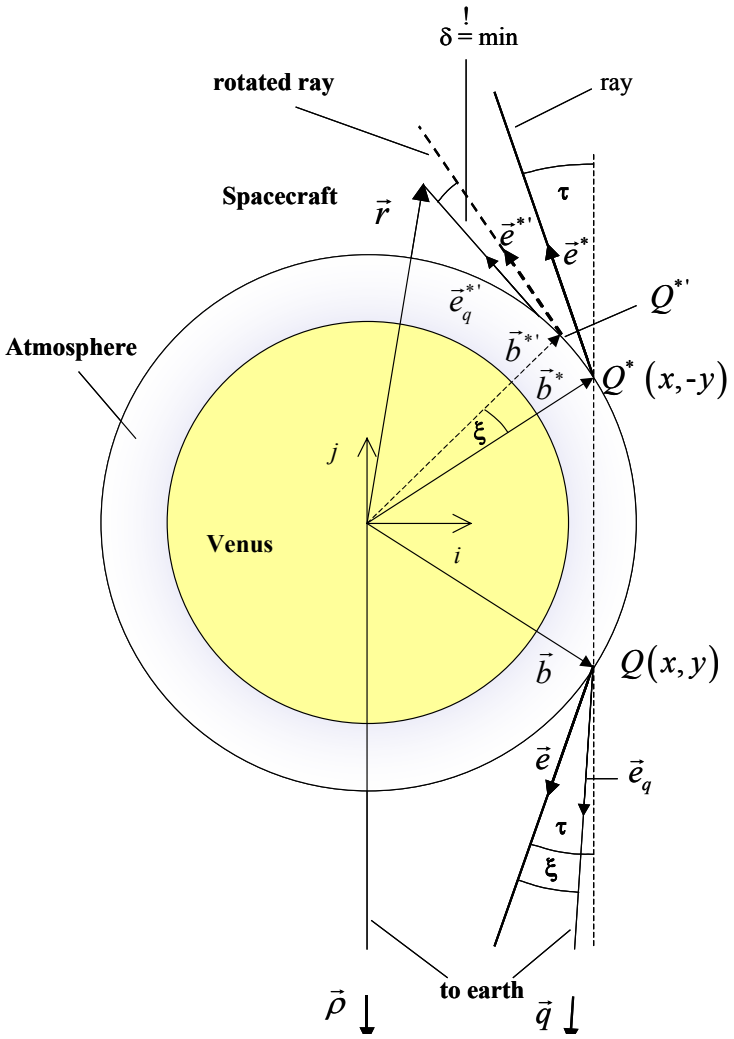

Figure 6-1: Ray path details

The radio signal is assumed to be emitted by the spacecraft in the upper hemisphere and to have a direction parallel to the $-\vec{j}$ direction after having penetrated the atmosphere.

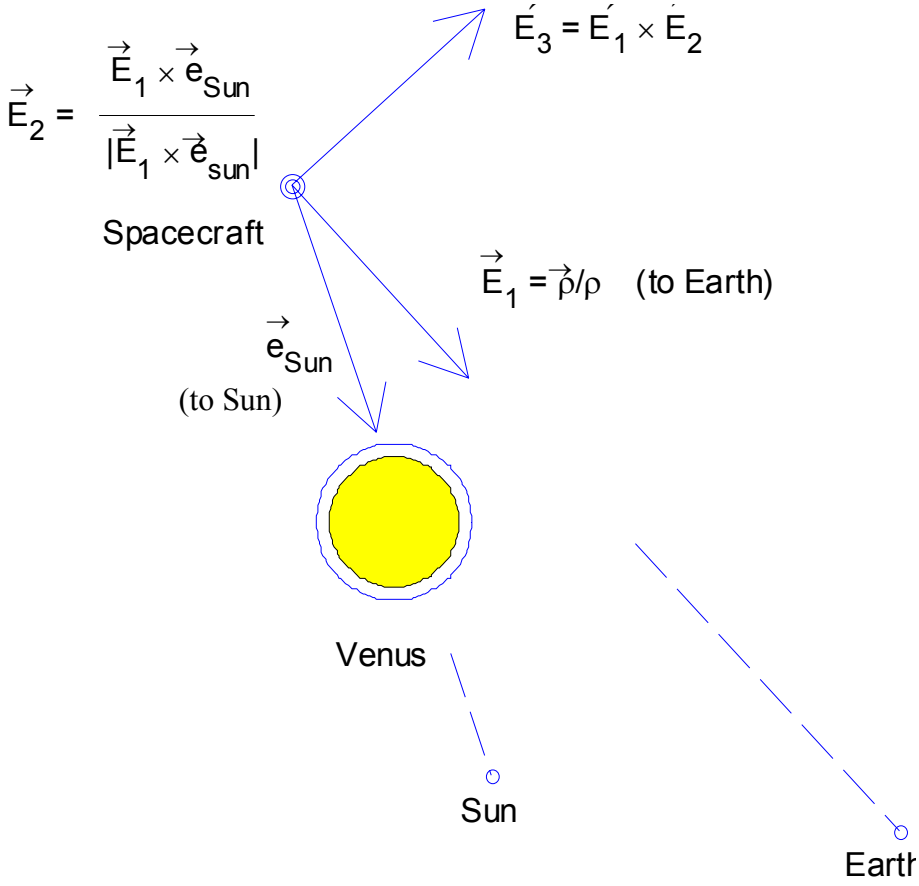

Fig. 6-2: Selected reference coordinate system

6.3.1 Numerical results for one pass (VEX orbit no. 215)

In the following, numerical results are given for one sample orbit (VEX orbit no. 215).

6.3.1.1 Orbital time

Julian date at beginning of occultation ($t = t_1$): JD = 2453972.467288789

beginning of occultation time t_1 = 0 s, $\theta = 259°$, orbit time: 23.3810 h (time mark o)

end of occultation time t_2 = 1 218 s , $\theta = 293°$, orbit time: 23.7198 h (time mark o)

6.3.1.2 Orbital elements

a = 39460.4909 km

e = 0.8337

i = 90.0766 °

Ω = 106.7088 °

ω = 103.4630 °

θ = 258.0953 ° (at $t = t_1$)

6.3.1.3 Coordinate system (J2000)

x-axis: $\vec{E}_1$ unit vector pointing from Venus to Earth at time t_1 (assumed as HGA boresight)

y-axis: $\vec{E}_2$ unit vector of $\vec{E}_1 \times \vec{e}_{sun}$

z-axis: $\vec{E}_3 = \vec{E}_1 \times \vec{E}_2$

$\vec{e}_{sun}$: unit vector pointing from Venus to Sun at time t_1

Attitude manoeuvres were determined with the constraint q_1 = 0, which implies no rotation of the S/C around the HGA axis during the attitude manoeuvre.

6.3.1.4 Chebyshev coefficients c_j

In the following we list the Chebyshev coefficients c_j for the quaternion $q = (q_1, q_2, q_3, q_4)$, degree N = 6.

j	$c_j^{(1)}$ for q_1	$c_j^{(2)}$ for q_2	$c_j^{(3)}$ for q_3	$c_j^{(4)}$ for q_4
0	0	0.01399725699208	0.00724475615905	1.99988280340424
1	0	-0.00105767284252	0.00107802529027	-0.00000070238859
2	0	-0.00878251491468	-0.00495246017300	0.00008674736028
3	0	0.00061891071708	-0.00220234844195	0.00000222487702
4	0	0.00108134948393	0.00044905116295	-0.00003316329678
5	0	-0.00013864510015	0.00024691757287	-0.00000240115780

for time interval [*a, b*] = [t_1, t_2] = [0 1218] s.

6.3.1.5 Chebyshev approximation

$$q_k = \sum_{j=0}^{N-1} c_j^{(k)} T_j(t) - \frac{1}{2} c_0 \text{ for } a \le t \le b \text{ and } k = 1, 2, 3, 4.$$

Note: No rotation around *x*-axis

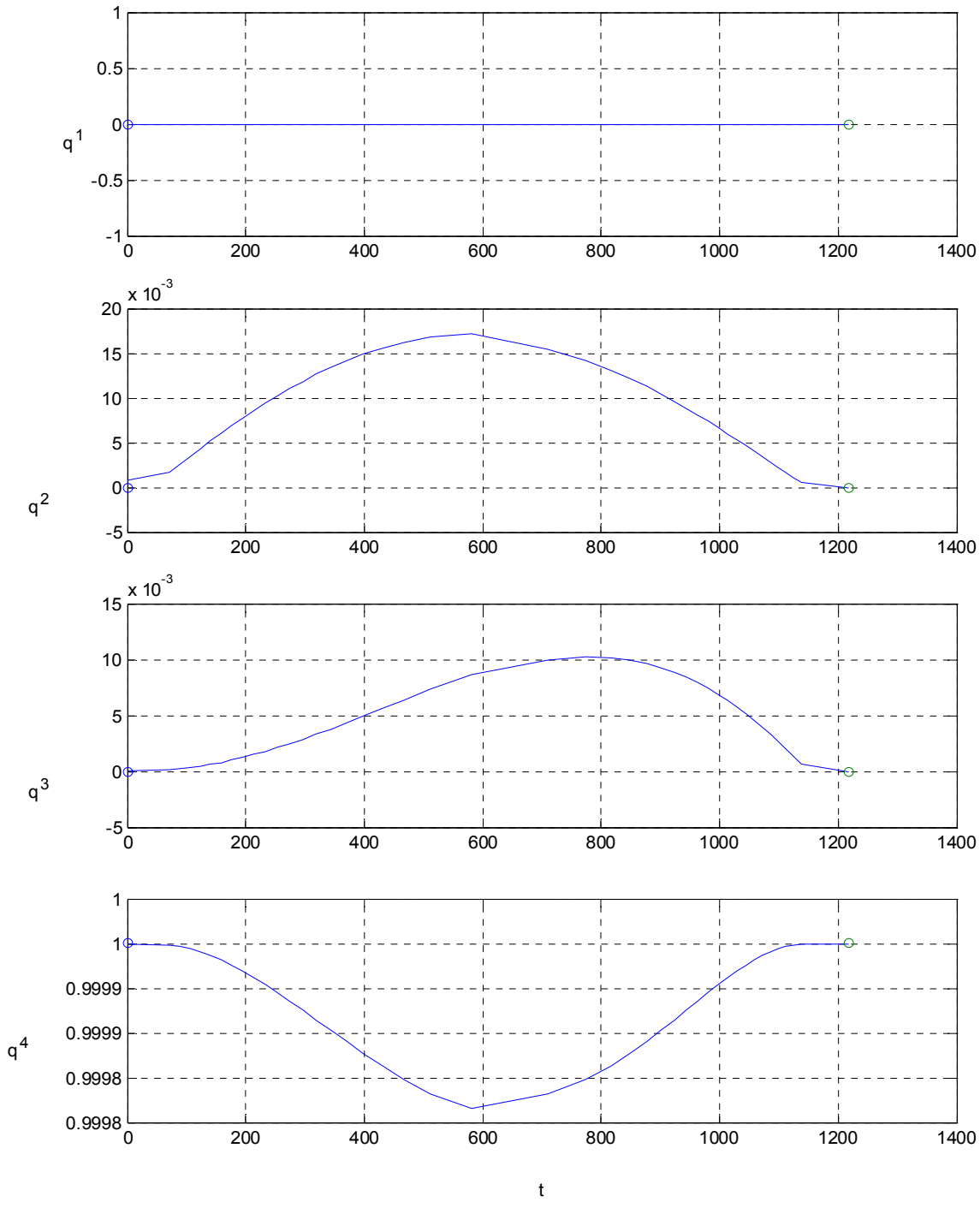

Fig. 6-3: Quaternions calculated from atmospheric/ionospheric density profiles (o marks beginning and end of occultation)

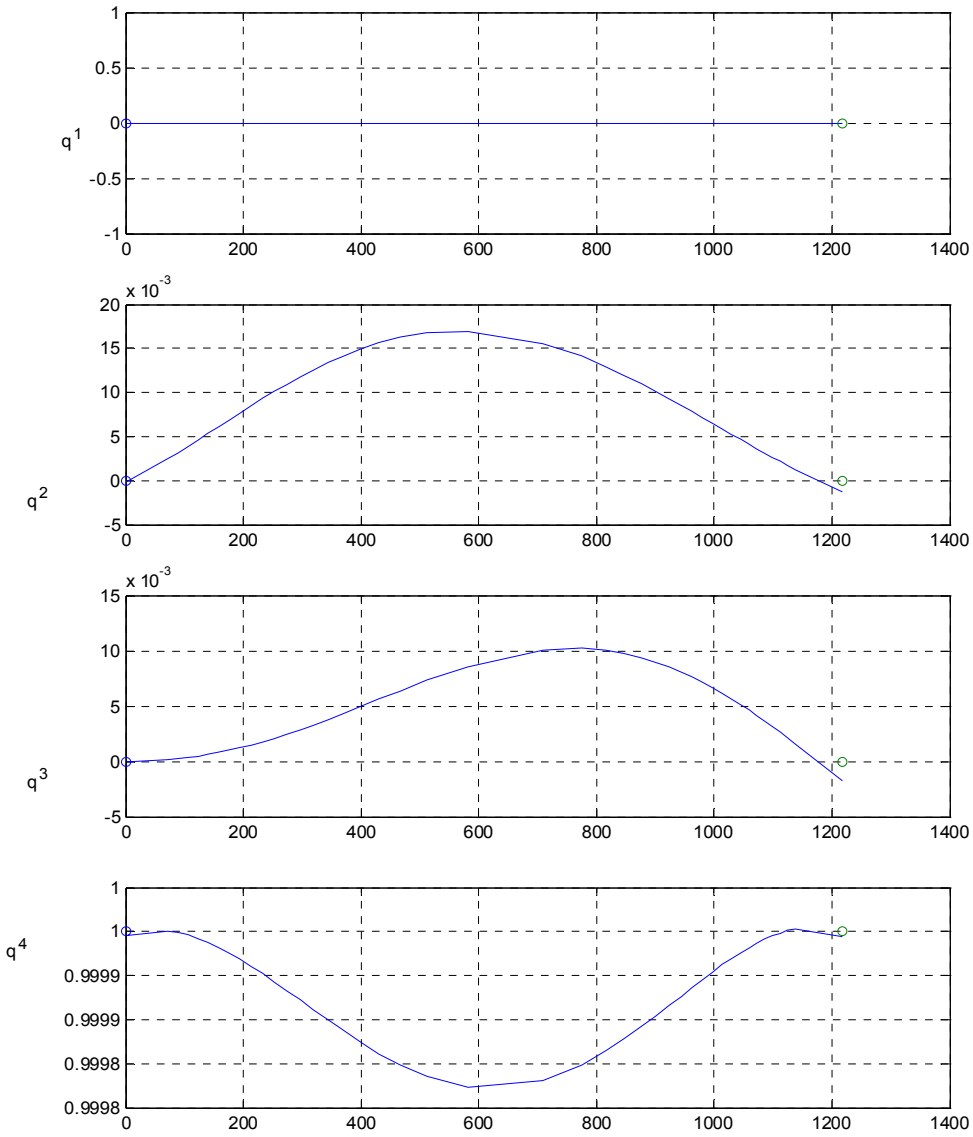

Fig. 6.4: Chebyshev approximation of quaternions from Fig. 6.3 (o marks beginning and end of occultation)

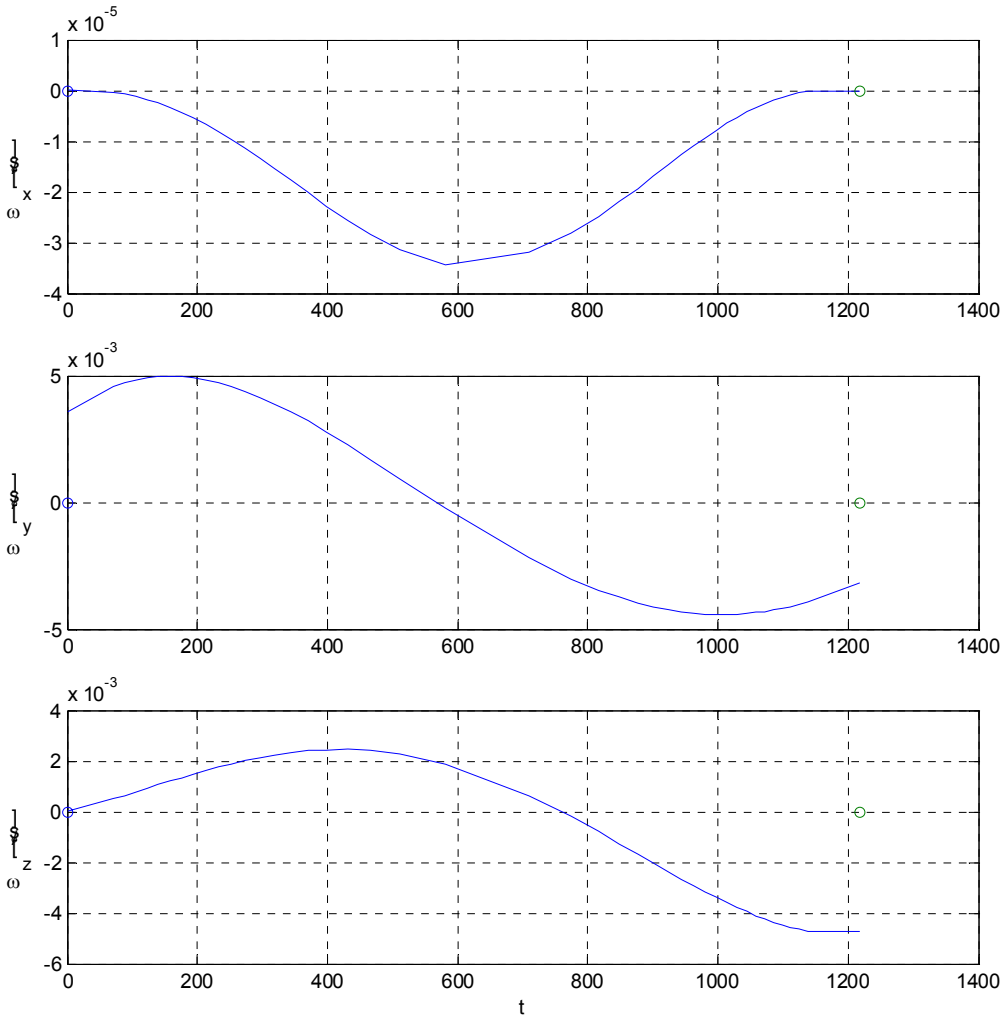

Fig. 6-5: Chebyshev approximation of $\vec{\omega}$ (o marks beginning and end of occultation), vector components given in the coordinate system defined above

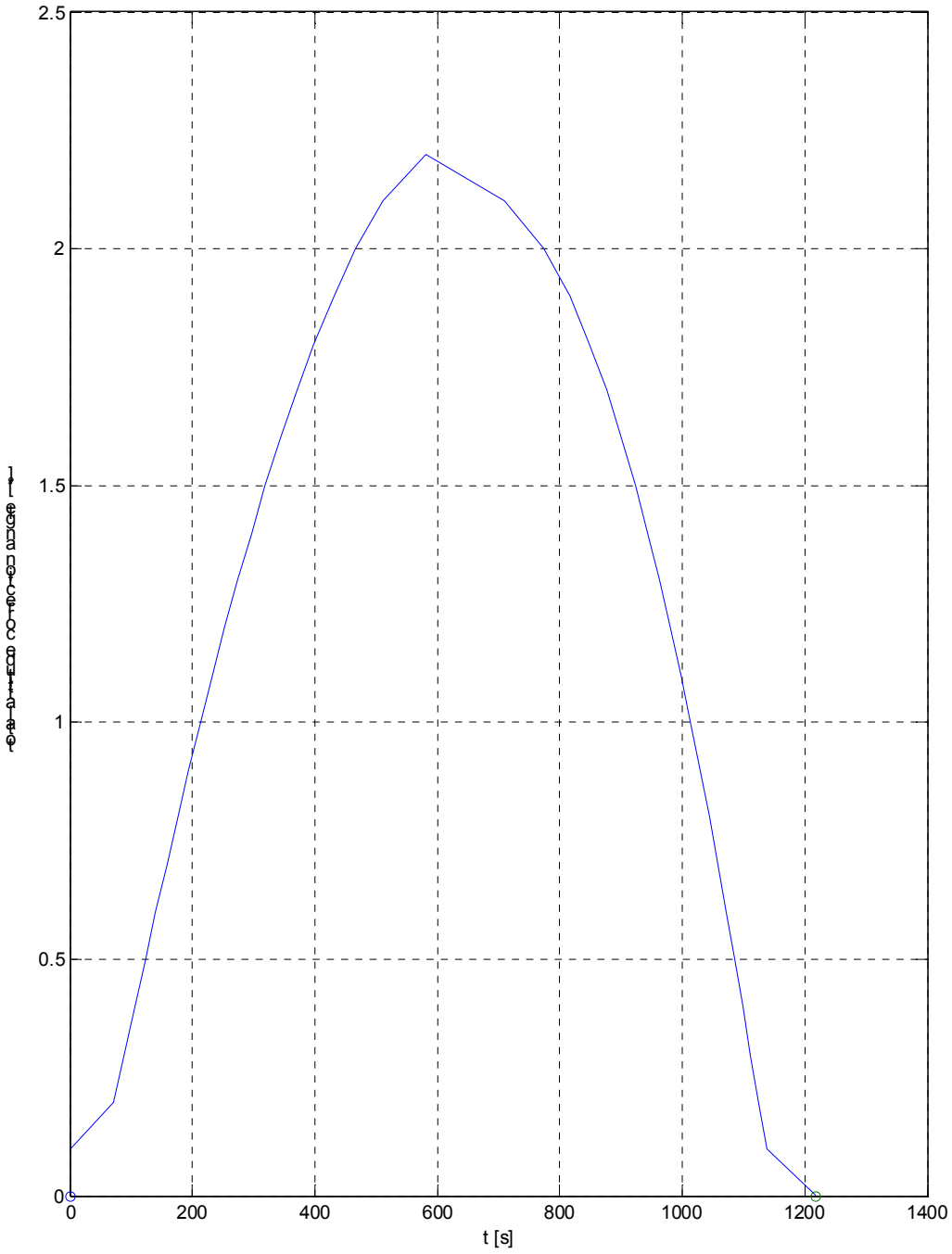

Fig. 6-6: Total attitude correction angle

For VeRa calibration purposes occultation experiment shall start with the HGA Earth pointing 15 minutes before beginning and shall end with the HGA Earth pointing 15minutes after end of physical occultation.

7. ADDITIONAL EFFECTS

7.1 Tropospheric Refraction of Earth Atmosphere

The effect of the neutral atmosphere is denoted as tropospheric refraction. The neutral atmosphere is a non-dispersive medium with respect to radio waves up to frequencies of 15 GHz. The refraction index n, however, is dependent on air pressure, temperature, humidity and zenith angle.

The effect is a delay that reaches 2.0 – 2.5 m in the zenith direction and increases approximately with the cosecant of the elevation angle, yielding about a 20 – 28 m delay at a 5° elevation angle independent on the frequency. The dependence of the delay on elevation angle and on humidity is illustrated in **Fig. 7.1-1.**

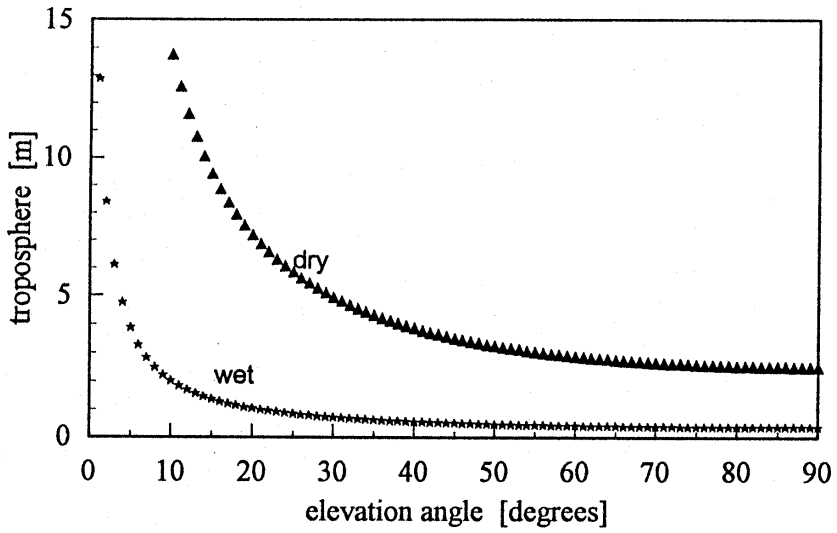

Fig. 7.1-1 Dry and wet tropospheric model delays [7.1]

The tropospheric path delay is defined by

$$\Delta^{Trop} = \int (n-1)\, ds \tag{7.1}$$

When instead of the refractive index n the refractivity $N^{Trop} = 10^6 (n-1)$

is used so that equation (7.1) becomes

$$\Delta^{Trop} = 10^{-6} \int N^{Trop}\, ds \tag{7.2}$$

Hopfield proposed to separate the refractivity into a “dry” and “wet” part. We obtain for the refractivity N^{Trop}

$$N^{Trop} = N_d^{Trop} + N_\omega^{Trop} \tag{7.3}$$

The expression for the tropospheric refractivity is based on the following empirical formula which includes meteorological parameters

$$N^{Trop} = 77.624\ p\ [hPa] / T\ [K] + 371900\ e\ [hPa]/ (T\ [K])^2 - 12.92\ e\ [hPa]/ T\ [K] \tag{7.4}$$

where p denotes the total atmospheric pressure in hPa, e is the partial pressure of water vapor in hPa, and T is the surface temperature in Kelvin.

The dry atmosphere contributes about 90% of the total tropospheric refraction.

Surface temperature and surface pressure values can be taken from the meteo data set provided by the G/S. Humidity measurements have to be estimated according to meteorological models. The G/S (NNO) is not equipped with water vapor radiometer or radio sonde instruments.

However, Hoffmann - Wellenhof [7.2] mention that surface meteorological data should be used with caution (Surface layer biases, temperature inversion and convection effects). Occasionally, it might be better to use the standard atmospheric values rather than the locally measured values.

The atmospheric bending angle Δ E (´´) in the Earth´s atmosphere can be estimated to

$$\Delta E = N \cdot 10^{-6} \frac{1}{\tan E} [rad] \tag{7.6}$$

E is equivalent to the elevation angle of the G/S antenna. The term *mapping function* is used to describe the relation between the tropospheric delay at zenith and an arbitrary angle E above the horizon. Rough estimates are given in Table 7.2.

E(°)	1	3	5	7	10	15	20	30	40	50	70	90
ΔE(″)	1358	836	589	449	328	222	166	106	73	52	23	0
$\Delta\rho$(m)	58	34	23	17	13	9	7	5	4	3	2	2

Table 7.2: Tropospheric refraction [3.1].

The tropospheric range correction Δ_r which is composed of a dry and a wet contribution can be modelled according to [7.1] and with the formulas given in **Table 7.1.**

It should be mentioned that other models are also available such as for example the model from Saastamoinen [7.3] with improvements by Davis [7.4]. The mapping functions are also extensively discussed in Sovers [7.5]. It will be left to further discussions among the Radio Science team which model will be eventually used for prediction and data analysis.

The troposheric range correction Δ_r will lead additionally to a measurable Doppler effect since the total phase path length of the radio signal varies with time.

The equivalent Doppler velocity to be expected during a full day ground station tracking will be approximately +/- 20m/4hrs = 1.4 mm/s.

i=1	dry component $(h_1 \equiv h_d)$	i=2	wet component $(h_2 \equiv h_w)$
p	pressure in mb at height (h_p)	h_t	height of temperature meas. in km
T	temperature in degree Kelvin	h_h	height of humidity meas. in km
h_k	height of station. in km	h	humidity (%) at height h_h
h_p	height of pressure meas. in km	β	elevation angle
Δ_r	range correction (meter)		

$$a_e = 6378.137 \qquad x = T - 6.5(h_h - h_t) \qquad y = \frac{7.5(x - 273.15)}{237.3 + x - 273.15} \qquad e_0 = 0.0611 * h * 10^y$$

$$t_k = T + 6.5h_t \qquad e_m = 5.2459587 \qquad e_s = e_0 * \left(\frac{t_k}{x}\right)^{4e_m} \qquad t_e = T + 6.5(h_t - h_p)$$

$$p_{sea} = p(t_k / t_e)^{e_m} \qquad r_{sea} = (77.624 * 10^{-6} / t_k) * p_{sea}$$

$$\alpha_{1i} = 1 \qquad \alpha_{2i} = 4a_i \qquad \alpha_{3i} = 6a_i^2 + 4b_i \qquad \alpha_{4i} = 4a_i(a_i^2 + 3b_i)$$

$$\alpha_{5i} = a_i^4 + 12a_i^2 b_i + 6b_i^2 \qquad \alpha_{6i} = 4a_i b_i(a_i^2 + 3b_i) \qquad \alpha_{7i} = b_i^2(6a_i^2 + 4b_i)$$

$$\alpha_{8i} = 4a_i b_i^3 \quad ; \quad \alpha_{9i} = b_i^4 \quad ; \quad a_i = -\left(\frac{\sin\beta}{h_i - h_k}\right) \quad ; \quad b_i = -\frac{1}{2a_e} * \frac{\cos^2\beta}{(h_i - h_k)}$$

$$R_i = \sqrt{(a_e + h_i)^2 - (a_e + h_k)^2 \cos^2\beta} - (a_e + h_k)\sin\beta$$

$$h_d = (1.1385 * 10^{-5} / r_{sea}) \qquad h_w = 1.1385 * 10^{-5}[(1255 / t_k + 0.05) / r_{sea}]$$

$$N_1 = r_{sea}\left(\frac{h_d - h_k}{h_d}\right)^4 \qquad N_2 = \frac{\left(\frac{0.371900}{t_k} - 12.92 * 10^{-6}\right)}{t_k} * e_s * \left(\frac{h_w - h_k}{h_w}\right)^4$$

$$\Delta_r = 10^3\left[N_1 \sum_{j=1}^{9} \frac{\alpha_{j1}}{j} R_1^j + N_2 \sum_{j=1}^{9} \frac{\alpha_{j2}}{j} R_2^j\right]$$

Table 7.1: Tropospheric Correction [7.1]

7.2 Ionospheric Refraction of Earth Ionosphere

The effect of the ionosphere is denoted as ionospheric refraction. The principles have been described in section 2.4. The ionosphere is a dispersive medium with respect to radio waves. The refraction index n is dependent on the electron number density profile which again depends on local time, and geomagnetic activity (see **Fig. 7.2-1**). The ionospheric refraction leads to a reduction in group velocity and an increase in phase velocity. The ionospheric correction can be selected to be active or non-active in the RSS routines.

The ionospheric range correction which can be described by applying a slant range factor (see Sovers [7.5] will lead additionally to a measurable Doppler effect since the phase ray path length of the radio signal varies with time.

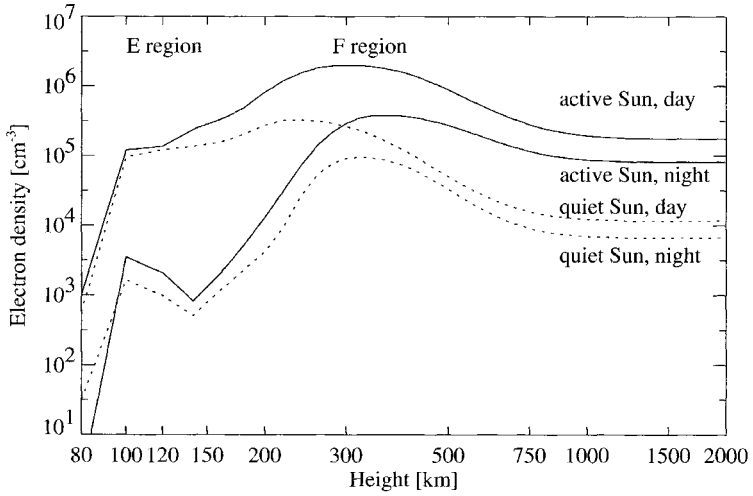

Fig. 7.2-1: Electron density profiles at mid latitudes based on the International Reference Ionosphere [7.7, 7.8]

The Doppler effects and the group delay can be determined according to the models based on GPS information (for example Klobuchar [7.6].

The effect is a delay that reaches typically 0.1 – 2ns (3 cm – 60 cm) in the zenith direction at 8.4 GHz. The dependence of the delay on electron density and frequency is illustrated in **Fig. 7.2-2**

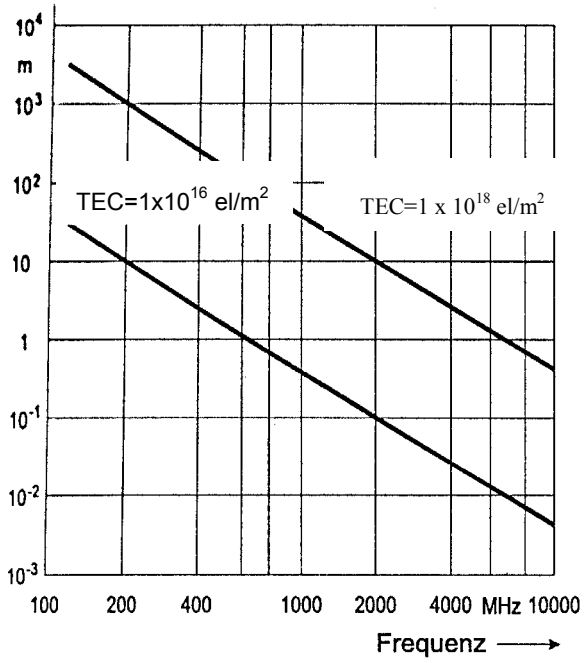

Fig. 7.2-2 Ionospheric delay as a function of frequency

7.3 Effects of General Relativity

We know from the laws of *General Relativity* that time is affected by gravitational potentials.

A radio frequency signal emitted at a specific gravitational potential Φ_1 is received with a different frequency when the receiver is located at Φ_2. Hence, when in the one way mode the G/S will receive a radio signal with a frequency different from the frequency when it was emitted.

The gravitational potential Φ is given by

$$\Phi = -\frac{GM}{r} \tag{7.3.1}$$

G and M being the gravity constant and the mass of the planetary object.

$GM_S = 1.33\ 10^{20}\ m^3\ s^{-2}$ (Sun) and $GM_E = 3.99\ 10^{14}\ m^3\ s^{-2}$ (Earth)

For small gravitational fiels ($|\Phi| << c^2$) we obtain:

$$(f_1 - f_2)/ f_2 = (\Phi_2 - \Phi_1)/c^2 = \Delta_f / f \tag{7.3.2}$$

If we simply take as an example the Venus and Earth orbit in the gravitational fiel of the Sun and neglect the individual masses of both planets we obtain for S-band and X-band the following relative frequency shifts:

Δ_f (S-band) = 8,7 Hz

Δ_f (X-band) = 31,6 Hz

In the two way mode the resulting frequency shift is negligible, because the frequency shift obtained in the uplink path is almost completely cancelled by the frequency shift obtained in the downlink path [2.14].

The incorporation of Doppler effects into the RSS was discussed in section 2.3.

The effect of General Relativity on the group delay observable was already discussed in section 2.6. It should be mentioned that the 2-way-delay can reach a maximum of 0.2 ms corresponding to an error of the observed TEC of 4×10^5 / 4×10^6 Hexems at S/X-band.

7.4 G/S Antenna and Receiver System

At beginning and end of each tracking pass the G/S internal group delay will be calibrated. These data will be incorporated in the scientific data analysis. Default values commonly agreed by ESA and the Radio Science team have to be included in the prediction analyses.

The G/S HGA antenna feed is also changing its position on the Earth's surface during a tracking pass. We can assume a variation of typically +/- 4m during a 8 hour period which is equivalent to a Doppler velocity of approximately 0.3 mm/s. The position data of the antenna feed as function of time must therefore also be included in the radio science simulation/analysis.

A further contribution to the ranging data arises because the radio wave is being reflected at the HGA subreflector before it enters into the antenna main feed system. The distance of this radio path is estimated to 4 m and its exact value has to be considered as additional group delay in the ranging data analysis (round trip). Details of the NNO antenna long loop ranging and calibration path delays are available in [7.9].

Details of corrections due to the G/S antenna structure and its motion are principally discussed in Sovers et al. [7.5]. A generalized schematic representation of the geometry of a steerable antenna is shown in **Fig. 7.4-1**.

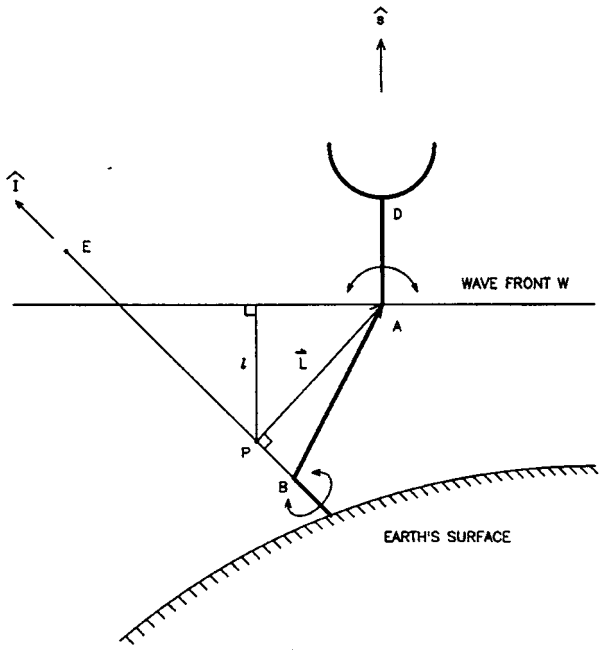

Fig. 7.4-1: Generalized schematic representation of the geometry of a steerable antenna. Two rotation axes and the "reference point" P are indicated. [7.5]

7.5 Onboard Transponder Delay

The transponder group delay effects will be measured by the ESOC and the Radio Science Team in the VEX project. These effects are of the order of 2 microseconds and depend strongly on S/C temperature. The modeling of these effects for both the prediction/simulation and the data analysis phase have to be commonly agreed upon by ESA/Astrium and the Radio Science Team.

8. SUMMARY AND CONCLUSIONS

a) We discussed time basis and reference coordinate systems which form the basis for the simulation, prediction and analysis of VeRa occultation experiments.

b) For these purposes the Radio Science Team developed a dedicated software simulator (RSS) based on MatLab/Simulink.

c) The JPL/DE 405 program is used to predict the planetary ephemeris data. The applicable time basis is TDB /T_{eph}. Events recorded at the VEX G/S use UTC as time basis. Appropriate relations exist to link the different time systems.

   Light travel time effects are included in the RSS routines

d) It was pointed out that details about the S/C onboard time OBT must be made transparent to investigate possible uncertainties in the onboard timing and data storage process.

e) The inertial coordinate system used is the J2000 system. Coordinates of the ground station are being calculated considering effects of precession, nutation, rotation and polar motion of the Earth.

f) Effects of General Relativity will have a substantial influence on the observables and are incorporated in the RSS.

g) We presented a mathematical method of ray tracing of microwave radio signals which penetrate the Venusian atmosphere/ionosphere. Dynamic S/C attitude manoeuvres – described by quaternions - which are necessary to compensate for atmospheric ray bending have been derived on the basis that the S/C performs no rotation about the HGA-axis. Further discussions are necessary with ESA/Astrium specifically on this subject. Also, further information describing the relation of the HGA coordinate system to the S/C coordinate system is required.

h) We discussed effects caused by the G/S antenna and receiver system and the S/C transponder. Coordination and exchange of information among the Radio Science team, ESA and Astrium is required.

i) We discussed effects of the troposphere and ionosphere of the Earth and presented various models which can be used to compensate for these effects. Also here, coordination and exchange of information among the Radio Science team and ESA is necessary.

9. REFERENCES

[1.1] Venus Express. An orbiter for the study of the atmosphere, the plasma environment, and the surface of Venus, ESA-SCI(2001)6, October 2001

[1.2] Venus Express Radio Science Experiment VERA, Technical Note, Science Performance Analysis, VEX-VERA-UBW-TN-3003, I.1.0, 25. 11. 2003

[2.1] VEX.AST.CO.0026, Venus Express Partnership Agreement, Issue 2, Rev 4, 01.07.03

[2.2] Eshleman, Von R., "The Radio Occultation Method for the Study of Planetary Atmospheres", Planet Space Sci., Vol. 21, pp.1521, 1973.

[2.3] Fjeldbo G., Eshleman V.R., Garriott O.K., Smith F. L. III, "The Two-Frequency Bistatic Radar-Occultation Method for the Study of Planetary Ionospheres", Journal of Geophysical Research, Vol. 70, No. 15, pp. 3701, Aug. 1965.

[2.4] Simpson R.A., "Spacecraft Studies of Planetary Surfaces Using Bistatic Radar", IEEE Trans. on GeoScience and RemoteSensing, Vol. 31 No. 2, march 1993.

[2.5] Bird, M.K., Coronal Investigations with occulted Spacecraft Signals. Space Science Reviews, 33, 99-126, 1982

[2.6] Muhleman, D.O., Anderson, J.D., Solar Wind Density from Viking Dual-Frequency Radio Measurements, Astrophys. Journ., 247, 1093-1101, August 1981

[2.7] Häusler, B., Radio Science Messungen im Sonnensystem mit einer Einführung in die Theorie der Gravitation, Forschungsbericht UniBwM, LRT-WE-9-FB-2 (2002)

[2.8] Hakim, R., An Introduction to Relativistic Gravitation, Cambridge Univ. Press, 1999

[2.9] Reasenberg, R.D., Shapiro, I.I., MacNeil,P.E., Goldstein, R.B., Breidenthal, I.C., Brenkle, J.P., Cain, D.L., Kaufman, T.M., Komarek, T.A., Zygielbaum, A.I., Viking relativity experiment: verification of signal retardation by solar gravity, Astrophys. Jour., 234, L219, 1979

[2.10] Iess, L., Giampieri, G.,Anderson, J.D., and Bertotti, B., Doppler measurement of the solar gravitational deflection, Class.Quantum Grav., 16, 1487-1502,1999

[2.11] Shapiro, I.I., Fourth test of General Relativity, Phys. Rev. Lett., 13, 789, 1964

[2.12] Krisher, T.P., Parametrized post-Newtonian gravitational refshift, Phys. Rev.D., 48, No. 10, 4639-4644,1993

[2.13] Krisher, T.P., Morabito, D.D., and Anderson, J.D., The Galileo Redshift Experiment, Phys. Rev. D, 70, No. 15, 2213-2216, 1993

[2.14] Schacke, R., Bestimmung des Dopplereffektes unter Berücksichtigung der Allgemeinen Relativitätstheorie am Beispiel der ESA- Missionen Bepi Colombo und Venus Express, Diplomarbeit Universität der Bundeswehr München, Institut für Raumfahrttechnik, 2002

[2.15] Schneider, M., Himmelsmechanik, Bd. III, Gravitationstheorie, Spektrum Verlag, 1996

[2.16] Soffel, M.H., Relativity in Astrometry, Celestial Mechanics and Goedesy, Springer Verlag, 1989

[3.1] Montenbruck, O., E. Gill, Satellite Orbits – Models, Methods and Applications, Springer, 1999

[3.2] R. Fisher, Astronomical Times, 1996
http://www.gb.nrao.edu/~rfisher/Ephemerides/times.html

[3.3] P. Seidelmann, Explanatory Supplement to the Astromical Almanac, Time (p. 43), 1992

(3.5) J. Rodrigues-Canabal, Zeitbasen-Time Basis, e-mail to B. Häusler Auhust 29, 2003

[3.6] Time Standards Overview, SOP-RSSD-TN-014, 2003

[3.7] Report of the IAU/IAG working group on cartographic coordinates and rotational elements of the planets and satellites: 2000 (2003)

[3.8] J. Meeus, Astronomische Algorithmen, Johann Ambrosius Barth, 2002

[3.9] Spacecraft Planet Instrument c-matrix Events (SPICE), NAIF/JPL,

[3.10] MEX Instrument Resource Analyser (MIRA)

[3.11] Mapping and Planning Payload Science, ESOC (MAPPS)

[3.12] Radio-Science-Simulator (RSS)

[3.13] Seidelmann, K., et al., Report of the IAU/IAG Working Group on Cartographic Coordinates and Rotational Elements of the Planets and Satellites, 2000; Celestial Mechanics and Dynamical Astronomy, 82, 83 - 110, 2002

[3.14] Seidelmann, P.K. and Fukushima,T., Why new time scales?, Astron.Astrophys.265, 833-838, 1992

[3.15] Vallado, D.A., Fundamentals of Astrodynamics and Applications, Kluwer Academic Publisher, 2001

[3.16] Mc Carthy, D.D., IERS Conventions, IERS, Technical Note No. 2; Central Bureau of IERS, Observatoire de Paris, 1996

[3.17] Seidelman, P.K., Abalakin, V.K., Bursa, M., Davies, M.E., De Bergh, C., Lieske, J.H., Oberst, J., Simon, J.L., Standish, E.M., Stooke, P. and Thomas, P.C., Report of the IAU/IAG Working Group on Cartographic Coordinates and Rotational Elements of the Planets and Satellites: 2000, Celestial Mech. and Dynam. Astronomy, Vol. 82, 83-110, 2002

[3.18] The Astronomical Almanac for the Year 2004, London, The Stationary Office B4, 2003

[3.19] Standish, E.M., Time Scales in the JPL and CfA ephemerides, Astron. Astrophys., 336, 381 – 384, 1998

[3.20] Diaz del Rio, J., Time Standards Overview, ESA, Planetari Missions Division, SOP-RSSD-TN-014, Issue 2, Rev. 1, 8 July 2003

[4.1] Lee, S.W., Magellan Venus Radio Occultation Atmospheric Profiles Data Set Archive, http://atmos.nmsu.edu/PDS/data/mg_2401]

[4.2] Fjeldbo, G. and Eshleman, V.R.: 1969, Radio Sci. 4, 879

[4.3] Howard, H.T. et. al.: 1974, Science 183, 1297

[4.4] Thayer, G.D., An improved equation for the radio wave refractive index of air, Radio Sci., 9, 803-807, 1974

[4.5] Eshleman, R., The Radio Occultation Method for the Study of Planetary Atmospheres, Planet. Space Sci., 1521, Vol.21, 1973

[4.6] Hupach, D. Berechnung des Leistungsverlustes von Signalen beim Durchleuchten der Atmosphäre von Planeten, Institut für Raumfahrttechnik der Universität der Bundeswehr München, Dezember 2002

[4.7] Kertz, W., Einführung in die Geophysik I/II, BI Hochschultaschenbuch, Mannheim, 1971

[7.1] Leick, A., GPS Satellite Surveying, Wiley, 1995

[7.2] Hofmann-Wellenhof, B. , Lichtenegger, H., and Collins, J., Global Positioning System, Theory and Practise, Springer, 1997

[7.3] Saastamoinen, J., Atmospheric Correction for the Troposphere and Stratosphere in Radio Ranging of Satellites, in Henriksen, The Use of artificial satellites for Geodesy, Geophys. Monogr. Ser., vol 15, 247-251, AGU, Washington DC, 1972

[7.4] Davis, J.L., Herring, T.L., Shapiro, I.I., Rogers, and Elgered, G., Geodesy by Radio Interferometry: Effects of Atmospheric Modelling Errors on Estimates of Baseline Length, Radio Science, Vol. 20, No. 6, pp. 1593 – 1607, Nov. – Dec. 1985

[7.5] Sovers, O.J. and Fanselow, J.L., Jacobs, C.S., Astrometry and geodesy with radio interferometry: Experiments, models, results, Rev. Modern Phys. Vol. 70, No. 4, 1393-1454, 1998

[7.6] Klobuchar, J.A., Ionospheric Effects on GPS, in: Global Positioning System: Theory and Applications, Vol I, ed. by Parkinson, B., Spilker, J., and Enge, P., American Inst. of Aeron. and Astron., 550 – 573, 1996

[7.7] Bilitza D., Rawer, K., Bossy L., Gulyaeva, T., International Reference Ionosphere-past, present, and future: I. Electron density; Adv. Space Res. 13/3, 3, 1993

[7.8] Bilitza, D., Koblinsky, C., Beckley, B., Zia, S., Williamson, R., Using IRI for the Computation of Ionospheric Corrections for Altimeter Data Analysis, Adv. Space Res. 15/2, 113-119, 1995.

[7.9] SED, Technical Note, Long Loop Ranging, Calibration Path Delay, Document 8410-116, Issue 1, June 27, 2002